AD_____

Award Number: DAMD17-01-1-0196

TITLE: The Role of Clusterin in Estrogen Deprivation-Mediated Cell Death in Breast Cancer Cells

PRINCIPAL INVESTIGATOR: Konstantin S. Leskov, Ph.D.
David A. Boothman, Ph.D.

CONTRACTING ORGANIZATION: Case Western Reserve University
Cleveland, Ohio 44106-7015

REPORT DATE: July 2003

TYPE OF REPORT: Annual Summary

PREPARED FOR: U.S. Army Medical Research and Materiel Command
Fort Detrick, Maryland 21702-5012

REPORT DOCUMENTATION PAGE

Form Approved
OMB No. 074-0188

1. AGENCY USE ONLY (Leave blank)	2. REPORT DATE	3. REPORT TYPE AND DATES COVERED
	July 2003	Annual Summary (4 Jun 02-3 Jun 03)

4. TITLE AND SUBTITLE
The Role of Clusterin in Estrogen Deprivation-Mediated Cell Death in Breast Cancer Cells

5. FUNDING NUMBERS
DAMD17-01-1-0196

6. AUTHOR(S)
Konstantin S. Leskov, Ph.D.
David A. Boothman, Ph.D.

7. PERFORMING ORGANIZATION NAME(S) AND ADDRESS(ES)
Case Western Reserve University
Cleveland, Ohio 44106-7015

E-Mail: Ksl9@po.cwru.edu

8. PERFORMING ORGANIZATION REPORT NUMBER

9. SPONSORING / MONITORING AGENCY NAME(S) AND ADDRESS(ES)
U.S. Army Medical Research and Materiel Command
Fort Detrick, Maryland 21702-5012

10. SPONSORING / MONITORING AGENCY REPORT NUMBER

11. SUPPLEMENTARY NOTES
Original contains color plates. All DTIC reproductions will be in black and white.

12a. DISTRIBUTION / AVAILABILITY STATEMENT
Approved for Public Release; Distribution Unlimited

12b. DISTRIBUTION CODE

13. ABSTRACT (Maximum 200 Words)

During the two years period, we demonstrated that human CLU gene produced at least two forms of CLU protein, secretory CLU and nuclear CLU that were made via alternative splicing mechanism. In the nCLU mRNA exon II that contains endoplasmic reticulum targeting sequence is spliced out resulting in a protein that remains in the cell and enters the nucleus after apoptotic signal. Inhibition of nCLU protein by siRNA in breast cancer cells resulted in higher resistance to ionizing radiation, suggesting that nCLU is a pro-apoptotic protein. Inhibition of sCLU resulted in higher radiosensitivity, indicating that sCLU is anti-apoptotic. Breast cancer cell line that lack estrogen receptor (ER) (T47D: C4:2W) had higher levels of nCLU than its ER-positive isogenic counterpart (T47D:A18) and was significantly more sensitive to IR. The effect of nCLU vs sCLU inhibition in breast cancer cell on their response to tamoxifen/estrogen ablation is currently under investigation. We are also studying human CLU promoter for the elements responsible for its activation by estrogen deprivation.

14. SUBJECT TERMS	15. NUMBER OF PAGES
Clusterin, Tamoxifen	22
	16. PRICE CODE

17. SECURITY CLASSIFICATION OF REPORT	18. SECURITY CLASSIFICATION OF THIS PAGE	19. SECURITY CLASSIFICATION OF ABSTRACT	20. LIMITATION OF ABSTRACT
Unclassified	Unclassified	Unclassified	Unlimited

Table of Contents

Introduction

Clusterin (CLU) is a protein which expression is associated with apoptosis in a number physiological processes, including mammary gland involution (1, 2, 3). CLU protein expression is induced after estrogen ablation/tamoxifen treatment. CLU protein exists in at least two forms, secretory CLU (sCLU) and nuclear CLU (nCLU). SCLU is thought to be cytoprotective (4) and nCLU – pro-apoptotic(2). During the first year of working on the Proposal, we concluded that nCLU protein in human breast cancer cells was translated starting at AUG-34 from the mRNA that is separate from that of sCLU. This nCLU mRNA is created by alternative splicing when exon II is omitted and exons I and II are spliced together (5). The loss of estrogen receptor correlated with higher level on nCLU protein (see previous Annual Report, 2002). We also showed that sCLU mRNA had a potential internal ribosome entry site (IRES) that resulted in a synthesis of an additional 41 kDa CLU form, which function was unknown.
Our working hypothesis is:
We hypothesize that the induction of nuclear clusterin (nCLU) in breast cancer cells results in higher apoptosis rate. We also hypothesize that the levels of nCLU and sCLU are the factors that determine the sensitivity of estrogen receptor-positive breast cancer cells to tamoxifen treatment. We also anticipate higher mammary carcinogenesis in clusterin knockout mice following DMBA treatment compared to wild-type or heterozygous animals, since potentially cancerous cells with heavily damaged genome are not eliminated by nCLU-dependent apoptosis in the CLU knockout animals.

Based on this hypothesis, we proposed a new Task 1.

a. Generate mammalian expression vectors containing human estrogen receptor (ER), ER interfering RNA (iRNA)-expressing system and nCLU iRNA-expressing system as described in [Paul, 2002 #498] (months 13-14).
b. Perform transfection of C4:2W cells with ER and nCLU iRNA plasmids, transfect T47D cells with ER iRNA plasmid. Select stable clones and confirm the expression of ER protein in C4:2W cells and down-regulation of nCLU protein in C4:2W ER protein in T47D. (months 14-22).
c. Determine cell growth response to estrogen and tamoxifen in the stably-transfected clones compared to vector alone transfectants. Determine the levels of Ku70 and Bax proteins and their intra-cellular distribution by Western blotting, and radiation sensitivity by clonogenic survival assay. (months 22-36).
d. Generate mouse monoclonal antibody toward the N-terminal part of nCLU (amino acids 34-114) (months 13-24).
e. Use anti-nCLU monoclonal antibody (depending on their quality and availability) to detect endogenous nCLU in T47D, C4:2W and MCF7:WS8 breast cancer cells following estrogen and tamoxifen treatments (months 24-36).

Progress and problems encountered.
During the first year of the funding period we found correlation between ER expression and nCLU protein production in ER-positive and –negative subclones of T47D breast cancer cells.

Since our data indicated that nCLU is a stress-induced death protein, we investigated whether the differences in steady-state levels of nCLU protein also correlate with breast cancer cell survival after clinically-relevant doses of ionizing radiation. Clonogenic survival assays were performed using T47D:C4:2W (C4:2D) and T47D:A18 (A18) cells (Figure 1). NCLU-overexpressing C4:2W showed significantly lower IR survival at all doses used compared to A18 cells that had low steady-state level of nCLU expression. To further investigate the relevance of nCLU and sCLU for IR survival, we employed siRNA technique to specifically inhibit nCLU and sCLU proteins in breast cancer cells. Two 19 bp RNA duplexes complementary to either exon I/exon III junction characteristic to the nCLU mRNA (5) or exon II that is present only in sCLU were synthesized (Dharmacon, Inc.) and transiently transfected into C4:2W cells. We expected increase in post-IR survival of the C4:2W cells with inhibited nCLU. However, no changes in nCLU levels following the transfection of anti-nCLU siRNA (sinCLU) were detected (data not shown). Subsequent transient transfections of siRNAs that had been shown to inhibit other targets, including Rb and SP1 proteins in different cell lines, did not show any effect in C4:2W, indicating that siRNA-mediated dicer system may not be functional in C4:2W, making it impossible to use as an experimental model.

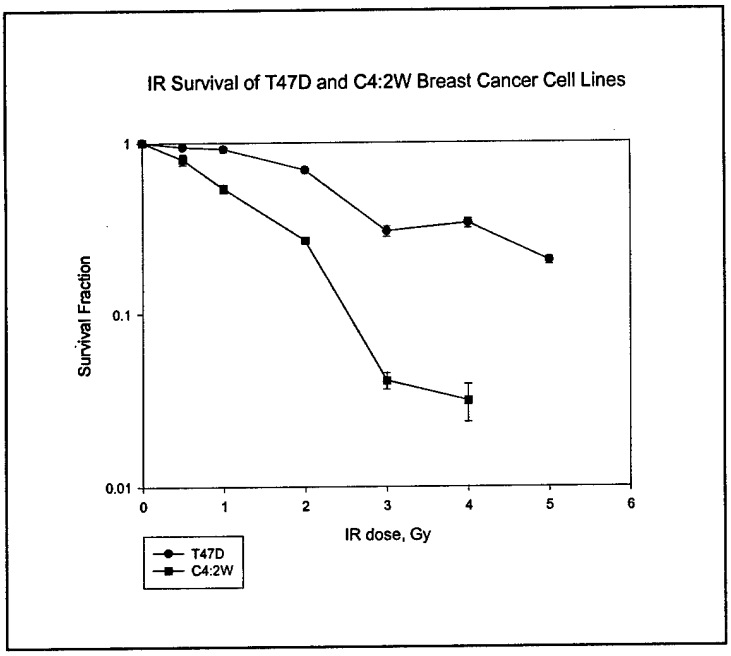

Figure 1. Estrogen-independent, nCLU-expressing C4:2W breast cancer cells exhibit lower radiation survival as compared to estrogen-dependent T47D breast cancer cells with low level of nCLU protein.

Instead of C4:2D, we used MCF-7 breast cancer cells to transiently inhibit nCLU protein using sinCLU siRNA. Unlike C4:2W, MCF-7 demonstrated detectable and specific changes in nCLU protein steady-state level 48 h after transfection with sinCLU as compared to mock-transfected cells and cells transfected with random 19 bp RNA duplex (Figure 2A). When subjected to various doses of IR 48 h post-transfection with sinCLU, MCF-7 cells showed significant increase in clonogenic survival as compared to the control transfected cells (Figure 2B). This strongly suggested that nCLU protein contributed to IR-induced cytotoxicity and might be a factor that determines breast cancer response to radiation therapy either alone or in combination with tamoxifen treatment. On the contrary, MCF-7 cells transfected with anti-sCLU

siRNA (sisCLU) demonstrated decreased IR survival (Figure 2C). Transfections with sinCLU and sisCLU were performed three times, in triplicates each. This indicated that sCLU and nCLU forms that result from alternative splicing have antagonistic functions. We are currently investigating the effect of the inhibition of nCLU and sCLU using sinCLU and sisCLU on the MCF-7 cell survival after either tamoxifen alone or IR/tamoxifen co-treatment. We expect that the inhibition of sCLU using sisCLU siRNA will lead to higher sensitivity to tamoxifen as compared to mock- or scrambled oligo-transfected cells. We anticipate that transfection with sinCLU will result in the increase of resistance to tamoxifen treatment.

A.

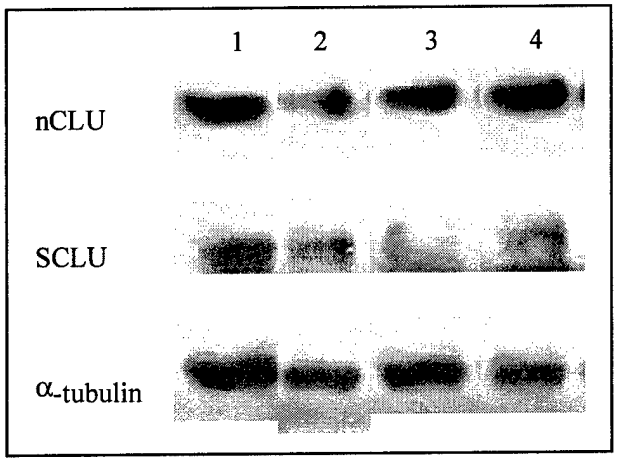

B.

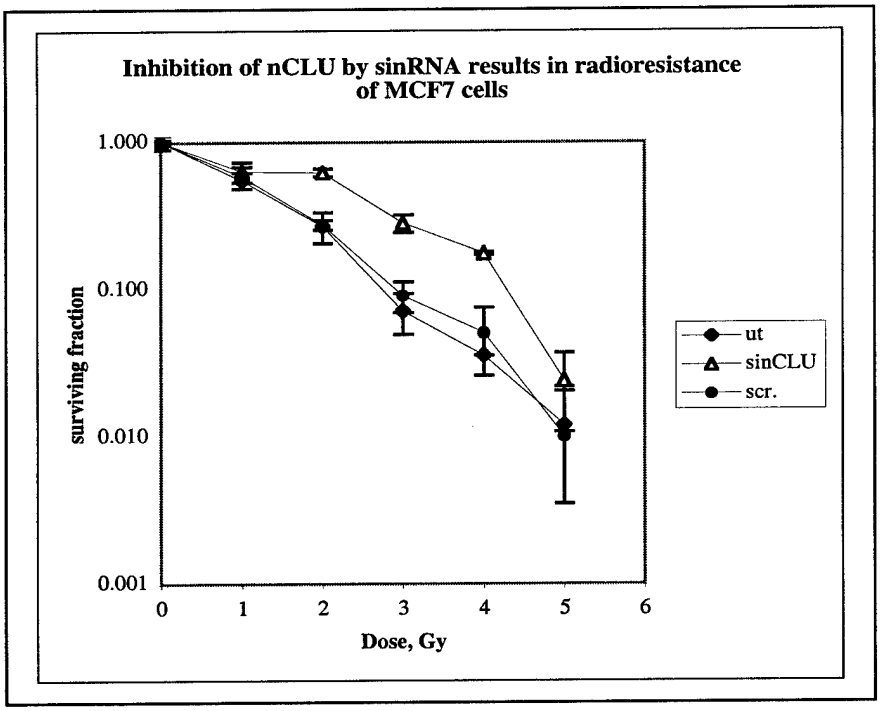

C.

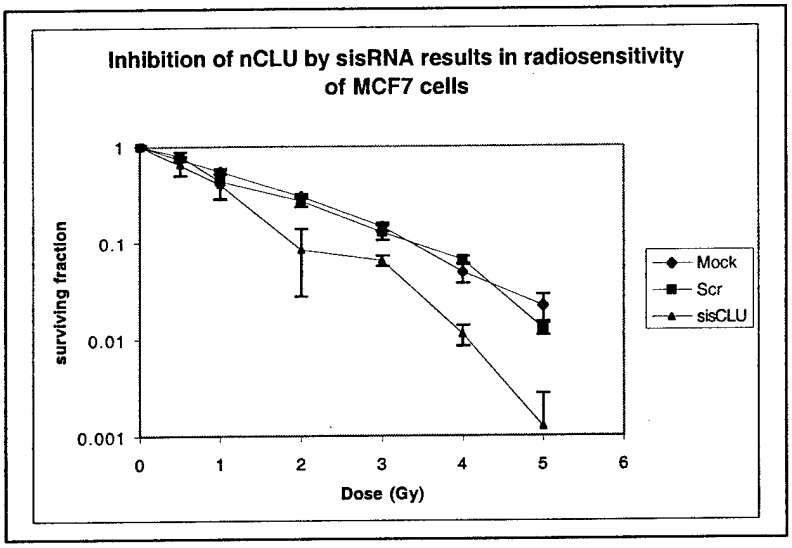

Figure 2. nCLU and sCLU protein forms have antagonistic functions in IR survival of MCF7 cells. **A.** Specific inhibition of nCLU and sCLU proteins using siRNAs. 1 - Mock transfected; 2 - sinCLU; 3 - sisCLU; 4 – scrambled double-stranded RNA oligonucleotide, harvest 48 h post-transfection. MCF7 cells transfected using Lipofectamine Plus (Invitrogen), 5 ug of each siRNA was used per well of 6-well plate. Western performed using H330 antibody (Santa Cruz) for nCLU, and B5 antibody (Santa Cruz) to detect p60 glycosylated form of sCLU. **B.** Post-IR clonogenic survival of MCF7 breast cancer cells either mock-transfected or transfected with scrambled RNA oligonucleotide or sinCLU. **C.** Post-IR clonogenic survival of MCF7 cells transfected with sisCLU vs scrambled RNA oligo- and mock-transfected cells.

Since currently available anti-CLU antibody, such as H-330 and B-5 (Santa Cruz Biotech) were not suitable to a number of proposed studies of the role of nCLU, we proposed to generate monoclonal nCLU-specific antibody. We made GST-fused human nCLU protein (GST-nCLU using pGEX-2T vector (Pharmacia). GST-nCLU protein was expressed in XL-Blue *E.coli*, purified using Glutathione-Sepharose (Pharmacia) and sent to the Monoclonal Antibody and Immunology Core Facility at Case Western Reserve University. The hybridoma cells producing nCLU-specific monoclonal antibody are currently being generated.

Task 2. Determine the ability of the N-terminal coiled-coil domain of clusterin to inhibit apoptosis caused by either estrogen deprivation or tamoxifen exposure.

Make a series of adenoviral vectors containing HA or HA-fused full-length clusterin, nCLU, N-terminal coiled-coil domain, central no-coil region, C-terminal coiled-coil domain and C-terminal no-coil region proteins (months 13-22).

Progress and problems encountered: We have made an adenoviral vector containing human nCLU cDNA with and without a mutation in the C-terminal coiled-coil domain. We have demonstrated by yeast two-hybrid assay that this mutation (Leu343 -> Pro, L343P) abrogates nCLU binding to Ku70. We hypothesize that L343P mutation may also abrogate apoptotic/cytostatic functions of nCLU. We transduced these adenoviral vectors into MCF-7 breast cancer cells. The levels of nCLU proteins however, did not change significantly in the transduced cells. We also did not see significant changes in clonogenic survival of the transduced MCF-7 cells.

Since we did not have positive data using nCLU in adenoviral vector, we propose to change Task 2 of the Statement of work. Since we have already studying the role of nCLU and sCLU in tamoxifen-induced growth arrest and apoptosis using siRNAs in Task1, we propose to investigate the regulation of CLU gene expression by tamoxifen in breast cancer cells on transcription level. We have previously shown that the activity of rat 315 bp CLU promoter measured using luciferase assay is significantly increased following estrogen deprivation (Figure 3A). The activity of human CLU promoter fragments from 1403 to 315 bp, however, did not show induction under the same conditions, despite detectable induction of the protein (Figure 3B). This suggests that the elements required for promoter activation by estrogen withdrawal are located either upstream of the 1403 bp fragment of human promoter or in the introns of human CLU gene. The 1403 bp fragment of human CLU promoter does not contain known estrogen-regulated elements. However, there are several potential transcription factor binding sites upstream of the 1403 bp region, including pregnane X receptor and progesterone receptor binding sites. We hypothesize that human CLU promoter is up-regulated by estrogen deprivation on the level of transcription and that the distal parts of its promoter contain transcription factor(s) binding sites that are responsible for CLU gene activation. To investigate this, we propose the following Task 2 (months 25-36).

a) Perform Northern blot analysis of CLU mRNA to detect changes in CLU mRNA steady-state levels with and without estrogen deprivation;
b) Isolate ~5000 bp fragment of human CLU promoter region, insert this fragment into a luciferase reporter vector (pGL3 Basic, Promega, Inc.);
c) Determine 5000 bp human CLU promoter activity with and without estrogen deprivation/tamoxifen treatment.
d) Perform deletion/site-directed mutagenesis analyses of the 5000 bp human CLU promoter to identify the element(s) required for its activation by estrogen deprivation/tamoxifen treatment.

A.

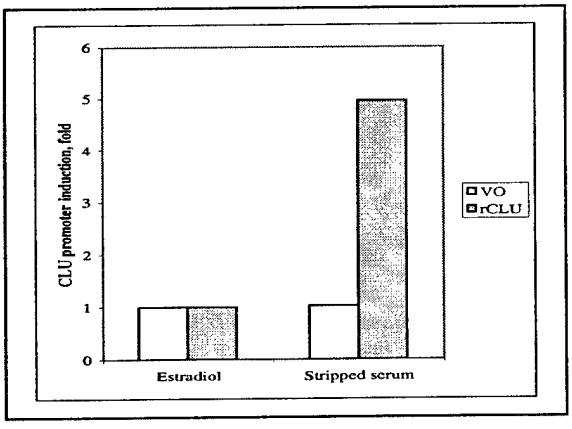

B.

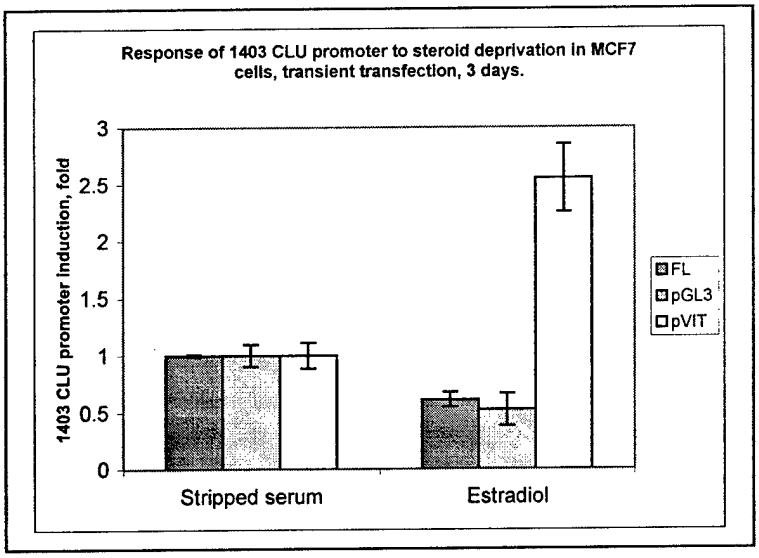

Figure 3. 315 bp fragment of rat CLU promoter, but not 1403 bp fragment of human CLU promoter is activated by estrogen deprivation. A. Rat CLU 315 bp fragment shows induction by estrogen deprivation; VO, vector only, rCLU, rat CLU promoter. B. Human 1403 bp fragment of CLU promoter does not show induction by estrogen deprivation. FL, 1403 bp fragment of human CLU promoter; pGL3, vector only; pVIP, positive control of luciferase reporter gene under the known estrogen-regulated promoter.

During the work on Task 2 we anticipate to determine whether human CLU promoter is activated by estrogen deprivation on transcription level and identify the elements required for CLU promoter activation by tamoxifen/estrogen ablation.

Task 3. Determine differences in oral DMBA-induced mammary gland tumorigenesis between clusterin knockout mice (-/-), compared to either heterozygous (+/-) or wild-type (+/+) animals.

Progress and Problems encountered: Our colony of CLU -/- mice stopped breeding for unknown reason. We are currently negotiating with Dr. Bruce Aronow to purchase new CLU -/- mice.

Key Research Accomplishments

- We determined that nCLU is produced in breast cancer cells by alternative splicing mechanism, i.e. by splicing together exon I and III;
- We demonstrated correlation between the status of estrogen receptor and nCLU expression;
- We developed siRNAs that specifically inhibit nCLU and sCLU protein expression;
- We determined that nCLU and sCLU have antagonistic functions regarding cell survival after ionizing radiation. This confirms our previous evidence that nCLU is pro-apoptotic and sCLU is anti-apoptotic;
- We performed structure/functional analysis of nCLU protein (see JBC paper in Appendix)

- We generated GST-nCLU fused construct and used it to produce nCLU antigen for the generation of monoclonal antibody.

Reportable outcomes.

During the second year of work on the Project the following abstracts submitted:

Konstantin S. Leskov, Jing Li, Dmitri Klokov and David A. Boothman. Synthesis of pro-apoptotic form of Clusterin in Breast Cancer cells. Era of Hope, DOD BCRP meeting, Orlando, September 25-28, 2002
Clusterin (CLU) is an ionizing radiation (IR)-induced protein that is reported to have both pro- and anti-apoptotic functions. The major form of the CLU protein is secreted (sCLU), and is induced by low doses of IR (>2 cGy). Several groups have shown that sCLU acts as a protector against apoptosis. The existence of another, nuclear form of CLU (nCLU) was proposed and reported by us (Yang et. al., PNAS, 2000). We demonstrated that nCLU induced caspase-3-independent cell death upon forced over-expression in MCF7:WS8 breast cancer cells. We also demonstrated that the C-terminal coiled-coil domain of nCLU was responsible for cell death. Our recent data indicate that the N-terminal coiled-coil domain of nCLU bound to the C-terminal coiled-coil domain, promoting either intra-molecular folding or oligomerization. We showed that endogenous nCLU protein was induced in the nuclei of IR-treated cells by higher doses of IR (1 Gy), and we hypothesized that nCLU protein induction may be necessary for the elimination of severely damaged cells. We recently determined the mechanisms for nCLU synthesis. We isolated a cDNA for nCLU from IR-treated MCF7:WS8 breast cancer cells. This nCLU mRNA was produced by splicing together exons I and III, and eliminating exon II, which contained the first AUG codon and the endoplasmic reticulum (ER)-targeting signal of sCLU. In the result of this alternative splicing, translation started from the second in-frame AUG codon positioned in exon III leading to the production of the nCLU protein. We are currently investigating the expression of nCLU in mammalian cells, its functions regarding apoptosis, and its responses to IR, including regulation of splicing and translation initiation. We propose that CLU RNA message undergoes alternative splicing resulting in pro- and anti-apoptotic form of the protein. We also explored nCLU expression in cells with different estrogen- and radiation sensitivities, interaction of nCLU with Ku70 and performed structure-function study of nCLU protein.

Konstantin S. Leskov, David A. Boothman. Biosynthesis and sub-cellular localization on nuclear clusterin (nCLU), 12th International Congress of Radiation Research, Brisbane, August 17-22, 2003 (to be presented).

The following peer-reviewed articles were published during 6/2002-7/2003:

Leskov, K, Klokov, DY, Li, J, Kinsella T J, and Boothman, DA. Synthesis and functional analyses of nuclear clusterin: a cell death protein. J. Biol. Chem. 278(13): 11590-11600, 2003. (Appendix)

Sun W., **Leskov K.S.**, Boothman, D.A, and Matsuyama, S., et al. Ku70 suppresses the apoptotic translocation of Bax to mitochondria. Nature Cell Biology 5(4): 320-329, 2003.

Non-peer-reviewed publication:

Criswell T., **Leskov K.S.**, Klokov D., Li J., and Boothman D.A. IR-induced transcriptional responses at clinically relevant doses. Oncogene, In Press, 2003.

Conclusions.

During the two years period, we demonstrated that human CLU gene produced at least two forms of CLU protein, secretory CLU and nuclear CLU that were made via alternative splicing mechanism. In the nCLU mRNA exon II that contains endoplasmic reticulum targeting sequence is spliced out resulting in a protein that remains in the cell and enters the nucleus after apoptotic signal. Inhibition of nCLU protein by siRNA in breast cancer cells resulted in higher resistance to ionizing radiation, suggesting that nCLU is a pro-apoptotic protein. Inhibition of sCLU resulted in higher radiosensitivity, indicating that sCLU is anti-apoptotic. Breast cancer cell line that lack estrogen receptor (ER) (T47D: C4:2W) had higher levels of nCLU than its ER-positive isogenic counterpart (T47D:A18) and was significantly more sensitive to IR. The effect of nCLU vs sCLU inhibition in breast cancer cell on their response to tamoxifen/estrogen ablation is currently under investigation. We are also studying human CLU promoter for the elements responsible for its activation by estrogen deprivation.

References

1. C. R. Yang, et al., *Nucleic Acids Res* **27**, 2165-74 (1999).
2. C. R. Yang, et al., *Proc Natl Acad Sci U S A* **97**, 5907-5912 (2000).
3. J. G. Leger, M. L. Montpetit, M. P. Tenniswood, *Biochem Biophys Res Commun* **147**, 196-203 (1987).
4. I. Viard, et al., *J Invest Dermatol* **112**, 290-6 (1999).
5. K. S. Leskov, D. Y. Klokov, J. Li, T. J. Kinsella, D. A. Boothman, *J Biol Chem* **278**, 11590-600. (2003).

THE JOURNAL OF BIOLOGICAL CHEMISTRY
Vol. 278, No. 13, Issue of March 28, pp. 11590–11600, 2003
Printed in U.S.A.

Synthesis and Functional Analyses of Nuclear Clusterin, a Cell Death Protein*

Received for publication, September 9, 2002, and in revised form, December 26, 2002
Published, JBC Papers in Press, January 24, 2003, DOI 10.1074/jbc.M209233200

Konstantin S. Leskov, Dmitry Y. Klokov, Jing Li, Timothy J. Kinsella, and David A. Boothman‡

From the Department of Radiation Oncology, Laboratory of Molecular Stress Responses, Ireland Comprehensive Cancer Center and Case Western Reserve University School of Medicine, Cleveland, Ohio 44106-4942

Nuclear clusterin (nCLU) is an ionizing radiation (IR)-inducible protein that binds Ku70, and triggers apoptosis when overexpressed in MCF-7 cells. We demonstrate that endogenous nCLU synthesis is a product of alternative splicing. Reverse transcriptase-PCR analyses revealed that exon II, containing the first AUG and encoding the endoplasmic reticulum-targeting peptide, was omitted. Exons I and III are spliced together placing a downstream AUG in exon III as the first available translation start site. This shorter mRNA produces the 49-kDa precursor nCLU protein. Ku70 binding activity was localized to the C-terminal coiled-coil domain of nCLU. Leucine residues 357, 358, and 361 of nCLU were necessary for Ku70-nCLU interaction. The N- and C-terminal coiled-coil domains of nCLU interacted with each other, suggesting that the protein could dimerize or fold. Mutation analyses indicate that the C-terminal NLS was functional in nCLU with the same contribution from N-terminal NLS. The C-terminal coiled-coil domain of nCLU was the minimal region required for Ku binding and apoptosis. MCF-7 cells show nuclear as well as cytoplasmic expression of GFP-nCLU in apoptotic cells. Cytosolic aggregation of GFP-nCLU was found in viable cells. These results indicate that an inactive precursor of nCLU exists in the cytoplasm of non-irradiated MCF-7 cells, translocates into the nucleus following IR, and induces apoptosis.

The clusterin (CLU)[1] gene was originally isolated by numerous laboratories due to its up-regulation during cell death responses in various tissues and after various toxic stress signals (1–11). CLU expression is complex, appearing as different forms in different cell compartments. One set of proteins is directed for secretion, and other CLU species are expressed in the cytoplasm and nucleus (see below). The secretory form of the clusterin protein (sCLU) has been extensively studied and is produced by translation from the first AUG codon of the full-length CLU mRNA. sCLU is targeted to the ER by an initial leader peptide. This ~60-kDa pre-sCLU protein is further glycosylated and proteolytically cleaved into α- and β-subunits, held together by disulfide bonds (12, 13). External sCLU is an 80-kDa protein that appears as an ~40-kDa α- and β-protein smear by SDS-PAGE under reducing conditions (14).

The role(s) of CLU in cell death processes is also complex and may be different for the various forms of the protein. Recent data suggest that overexpression of sCLU in human cancer cells caused drug resistance and protection against certain cytotoxic agents that induce apoptosis (9, 15, 16). Additional confirmatory data suggest that sCLU acts as a molecular chaperone, scavenging denatured proteins outside cells following specific stress-induced injury such as heat shock (17–21). In fact, sCLU possesses nonspecific binding activity to hydrophobic domains of various proteins *in vitro* (20), further supporting its role as a molecular chaperone acting to clear cellular debris. sCLU does not associate with Ku70 (14).

Other data, including our own (13), show that overexpression of a specific nuclear form of CLU (nCLU) acts as a pro-death signal, inhibiting cell growth and survival. Our laboratory isolated CLU while searching for Ku70-binding proteins using a yeast two-hybrid screen of a human liver cDNA library (14). The specificity of nCLU-Ku70 interaction was confirmed by co-immunoprecipitation, far Western, and confocal co-localization analyses of the two proteins in transfected or IR-treated MCF-7:WS8 (MCF-7) breast adenocarcinoma cells (13). Confocal microscopy revealed an apparently inactive form of nCLU (*i.e.* pnCLU) in the cytoplasm of non-irradiated cells (13) that subsequently translocated to the nucleus following clinically relevant low dose IR exposures (≥1Gy). Co-immunoprecipitation studies demonstrated the presence of the Ku80 protein in the Ku70-nCLU complex, strongly suggesting that nCLU bound to the Ku70/Ku80 dimer (13). Overexpression of nCLU also blocked Ku70/Ku80 DNA end binding activity (14); however, the relationship between nCLU binding to Ku70 and cell death remained undetermined.

Interestingly, an ~49-kDa nuclear CLU precursor (pnCLU) was induced and translocated from the cytoplasm to the nucleus after certain cytotoxic events, including IR (13) or transforming growth factor-β (22) treatments. This "death" form of the CLU protein was proposed to be synthesized from a second in-frame AUG codon (13, 22), although mechanisms of production were not elucidated. The pnCLU protein apparently lacks the ER-targeting leader peptide and does not undergo α/β cleavage or extensive glycosylation, as observed with sCLU (22). pnCLU functions remain unknown. Following IR treatment of MCF-7 cells, an ~55-kDa nCLU protein was expressed

* This work was supported by NCI Grants CA78530 (to D. A. B.) and CA84578 (to T. J. K.) from the National Institutes of Health and by the Department of Defense Breast Cancer Research Program DAMD17-01-1-0196 (to K. S. L.). The costs of publication of this article were defrayed in part by the payment of page charges. This article must therefore be hereby marked "*advertisement*" in accordance with 18 U.S.C. Section 1734 solely to indicate this fact.

‡ To whom correspondence should be addressed: Dept. of Radiation Oncology (BRB-326 East), Laboratory of Molecular Stress Responses, Case Western Reserve University, 10900 Euclid Ave., Cleveland, OH 44106-4942. Tel.: 216-368-0840; Fax: 216-368-1142; E-mail: dab30@po.cwru.edu.

[1] The abbreviations used are: CLU, clusterin; aa, amino acid; nCLU, nuclear clusterin; sCLU, secreted clusterin; pnCLU, precursor of nuclear clusterin; GFP, green fluorescent protein; GST, glutathione sulfotransferase; MCF-7, MCF-7:WS8; IR, ionizing radiation; ER, endoplasmic reticulum; N-term, N-terminal domain of nCLU (aa 18–97); Center, central region of nCLU (aa 98–317); Ccoil, C-terminal coiled-coil region of nCLU (aa 318–368); End, C-terminal non-coiled coil region of nCLU (aa 367–448); NLS, nuclear localization signal; X-gal, 5-bromo-4-chloro-3-indolyl-β-D-galactopyranoside; RT, reverse transcriptase; ER, endoplasmic reticulum; Gy, gray.

at extremely low levels in the nuclei of exposed cells (13). Overexpression of GFP-fused nCLU (initiated from the second AUG start codon in its mRNA) or a C-terminal 120-amino acid fragment (C-120) in MCF-7 cells resulted in significant growth inhibition, caspase 3-independent apoptosis, and lethality (13, 23). All attempts to stably express nCLU resulted in lethality (13) or clones expressing G418 resistance without nCLU.[2] In contrast, overexpression of sCLU protein did not affect the survival of MCF-7 cells before or after IR stress (14).

Analyses of the amino acid sequence of full-length rat CLU detected four "myosin tail-like" domains (24) that are synonymous with a "coiled-coil" structure. Coiled-coil domains are the most common motifs used by proteins for oligomerization, and consist of amphipathic α-helices usually with a 4-3 pattern of hydrophobic and hydrophilic residues repeated in heptads. To date, no structure/function studies of the CLU protein have been performed, and mechanisms of the production of nuclear forms of this protein has yet to be determined.

The objectives of the following studies were as follows: (*a*) investigate the mechanism(s) of nCLU production; (*b*) identify the functional NLS of the protein; (*c*) identify the death domain of nCLU, and (*d*) elucidate the Ku70-binding domain of nCLU. These studies may then allow elucidation of the role of nCLU-Ku70 binding in cell death responses. We demonstrate that nCLU has one high affinity coiled-coil Ku70 binding domain within its C terminus. This domain is essential for its cell death function. Furthermore, nCLU contains an additional coiled-coil domain in its N terminus that interacts with its own C-terminal coiled-coil domain. Interestingly, the N-terminal coiled-coil domain of nCLU does not interact with Ku70. Furthermore, an N-terminal nCLU coiled-coil-containing peptide interfered with binding of the nCLU C-terminal coiled-coil domain with Ku70. Based on the apparent physical interactions of N- and C-terminal pnCLU coiled-coil domains, we offer a mechanism by which the inert ~49-kDa pnCLU could become activated to an ~55-kDa nCLU death protein. Finally, we discuss the cell death function of nCLU in damaged cells, and we propose mechanisms of cell death involving Ku70 binding.

EXPERIMENTAL PROCEDURES

RT-PCR of nCLU—Based on probable splice sites, the following primers were used to investigate whether alternative splice forms of CLU could be found: hCLU5′, 5′-ACAGGGTGCCGCTGACC-3′; hCLU-N-term-rev, 5′-TTAGAGCTCCTTCAGCTTTGTCTC TG-3′; NCLU-forw-3, 5′-GCTGACCGAAATGTC-3′; hnCLUrev, 5′-TCACACCACCC-GGTGCTTTTTG-3′. Total RNA from MCF-7 cells was extracted using RNAsol B (Invitrogen). Reverse transcription reactions were performed using the oligo(dT) primer (Promega) and Superscript II enzyme system (Invitrogen). The PCR step was performed using *Taq* DNA polymerase (Invitrogen). When hCLU5′ and hCLUN-term-rev primers were used, PCR conditions were as follows: 95 °C for 30 s, 62–72 °C for 45 s, and 72 °C for 45 s. When NCLUforw-3 primer was used in pair with either hCLUN-term-rev or hnCLUrev primers, optimal conditions were as follows: 95 °C for 30 s, 64 °C for 45 s, and 72 °C for 45 s. A Bio-Rad iCycler Thermal Cycler was used for all reactions. RT-PCR products were resolved by 2% agarose gel electrophoresis and purified using the Concept Matrix Gel Extraction System (Invitrogen). DNA sequencing was performed by the Case Western Reserve University DNA Sequencing Service.

Computer Analyses of Protein and Nucleic Acid Primary and Secondary Structures—EMBnet software (www.ch.embnet.org/software/COILS_form.html) was used to analyze amino acid (aa) sequences of mouse and human CLU proteins for coiled-coil domain structures; coiled-coil domains in proteins are known to be important for protein-protein interactions (25–27). Analyses were performed using the algorithm published by Lupas *et al.* (28). Primary sequences of both human and mouse CLU proteins were retrieved from GenBank™ (accession numbers: S70244 for mouse and M64722 for human CLUs (12, 29)). Construction of PCR primer sets for deletion/mutation analyses of the CLU protein was performed using OligoTech version 1.00 software (Oligos Etc., Inc./Oligos Therapeutics, Wilsonville, OR).

Generation of CLU Mutants and Yeast Two-hybrid Analyses—The Y190 yeast strain (HIS3,*lacZ*,*trp1*,*leu2* (30, 31)) was used in two-hybrid structure/function analyses as described (13, 14). Full-length mouse CLU cDNA was a generous gift from Dr. M. Tenniswood (Notre Dame University). Full-length mouse Ku70 cDNA was a generous gift from Dr. M. Abe (National Institute of Radiological Sciences, Japan). Human CLU and Ku70 constructs were used as described previously (14). Mouse CLU deletion mutants, containing aa residues 18–448, 18–97, 98–317, 18–380, 18–328, 256–328, 345–380, and 318–368, and human CLU deletion fragments 34–449 and 245–380 were created by PCR using the appropriate primer sets (described above). Deletion mutants were inserted into either pAS2-1 or pACT2 vectors (Clontech Laboratories, Inc., Palo Alto, CA) as prey or bait, respectively, using *Sma*I sites and the Perfectly Blunt™ Cloning kit (Novagen, Inc., Madison, WI), according to manufacturer's instructions. Mouse CLU deletion mutants containing amino acids 256–448, 256–380, and 256–344 were created using *Nco*I restriction enzyme digestion in combination with *Bam*HI, *Sca*I, or *Pst*I, respectively. The resulting fragments were then inserted into the pAS2-1 vector using *Nco*I, *Bam*HI, *Sma*I, and *Pst*I restriction sites. Mouse Ku70 cDNA was excised from the original vector using *Bsp*LU11I and *Eco*RI enzymes, and inserted into pACT2 and pAS2-1 vectors, which were pre-digested with *Nco*I and *Eco*RI restriction enzymes. Point mutations within mouse CLU cDNAs were introduced using the QuikChange kit (Stratagene, Cedar Creek, TX) following the manufacturer's instructions. The LR mutant (substitution of 9 Leu residues to Arg within the C-terminal coiled-coil domain of mouse nCLU) was generated by direct cloning of a 155-bp DNA fragment containing all required nucleotide substitutions. This was accomplished by first synthesizing a single strand DNA fragment: 5′ GC CAG GAG CGG AAC GAC TCG CGC CAG GTG GCC GAG AGG CGGACA GAG CAG TAC AAG GAG CGG CGG CAG TCC TTC CAG TCG AAGATG CGC AAC ACC TCA TCC CGG CGG GAG CAG CGG AAC GAC CAGTTC AAC TGG GTG TCC CAG CGG GCT AAC CGC A 3′. This fragment was further amplified by PCR using *Pfu* DNA polymerase (Stratagene, Cedar Creek, TX) and the following pair of primers: AlmutPCR1 (30-mer), 5′ GCT AAC CTG CGC CAG GAG CGG AAC GAC TCG 3′, and AlmutPCR2 (38-mer), 5′ TTA GTA GTA CTT GTC TTC TCC CTG TGT GCG GTT AGC CC 3′.

The PCR product was gel-purified, digested with the *Eco*NI restriction enzyme, and inserted into the pASnCLU, pAS-(256–448) and pGFPnCLU nCLU vectors, which were pre-digested with *Eco*NI to create NCLU-LR, *Nco*LR, and GFP-NCLU-LR, respectively. In addition, the undigested PCR product was inserted into a pcDNA3.1/NT-GFP-TOPO mammalian expression vector (Invitrogen) using blunt ligation to create the GFP-CcLR mutant.

Human CLU cDNA fragments encoding aa residues 84–449 and 329–449 in the pACT2 vector, as well as human Ku70 cDNA in the pAS2 vector, were described previously (13, 14). All constructs were sequenced to verify in-frame positions with respect to the GAL4 domain. GAL4-Ku70 was co-transfected with various GAL4-CLU fragments into Y190 yeast using the protocol provided in the MATCHMAKER (Clontech Laboratories, Inc., Palo Alto, CA) manual. Stable transformants were grown for 6 days at 30 °C on plates containing His(−), Trp(−), Leu(−) and SD medium (Difco) containing 2% agarose and 15 mM 3-amino-1,2,4-triazole. Colonies were subjected to on-filter β-galactosidase assays, with X-gal as a substrate. The reaction was considered positive when colonies turned blue within first 120 min of incubation with X-gal. Negative reactions (*i.e.* blue colonies were not observed) were indicative of no association, only when protein expression for each CLU or Ku70 mutant could be demonstrated by Western blot analyses (see below). Blue colonies that appeared after 120 min were regarded as false-positive signals. X-gal staining was performed on colony-lift filters as described (14).

Western Blot Analyses—Rabbit polyclonal H-330 antibody (Santa Cruz Biotechnology) was used to detect the 49-kDa species of CLU (pnCLU) in whole cell extracts from MCF-7 cells. A 1:2500 dilution of primary H-330 antibody was used followed by 1:10,000 dilution of horseradish peroxidase-conjugated anti-rabbit secondary antibody (Santa Cruz Biotechnology).

Yeast extracts were prepared using acid-washed glass beads as described in the MATCHMAKER kit manual and were used for Western blot analyses. Protein concentrations were determined using the Bio-Rad protein concentration reagent as per manufacturer's instructions (Bio-Rad). Yeast extracts were mixed with an equal volume of 2× Laemmli buffer, boiled for 5 min, and resolved on either 10 or 15%

[2] C.-R. Yang, K. S. Leskov, and D. A. Boothman, unpublished observations.

PAGE gels, depending on the expected molecular weight of the proteins of interest. Proteins were then transferred onto polyvinylidene difluoride-Plus membranes (MSI, Westboro, MA). Membranes were blocked with 5% non-fat dried milk and probed with anti-GAL4BD or anti-GAL4AD monoclonal antibodies (Santa Cruz Biotechnology, Inc., Santa Cruz, CA). Horseradish peroxidase-conjugated anti-mouse secondary antibody (Amersham Biosciences) was then used, and proteins were visualized by ECL (Amersham Biosciences) and x-ray film. All CLU deletion or point mutants were approximately equally expressed in yeast, and no loss of stability of proteins was noted.

In Vitro GST-Ku70 Binding Assays—Full-length mouse Ku70 cDNA was amplified using PCR and the appropriate primer sets and inserted into the pGEX-2T vector (Amersham Biosciences) at a *Sma*I restriction site to generate an in-frame glutathione *S*-transferase (GST)-fused protein. *Escherichia coli* NovaBlue Single Competent Cells (Novagen, Inc., Madison, WI) were used for plasmid propagation according to the protocol described in the Perfectly Blunt™ Cloning kit manual (Novagen, Inc., Madison, WI). GST or GST-Ku70 fusion proteins were generated and purified using standard methods (32). All genetically manipulated plasmids were confirmed by DNA sequencing prior to use. Glutathione-agarose beads (Amersham Biosciences) were used for purification of GST-fused proteins as described (32) using Binding buffer (20 mM Tris-HCl, pH 7.2, 150 mM NaCl, 1.5 g/liter bovine serum albumin, proteinase inhibitors). Amounts of immobilized GST-Ku70 or GST (alone) proteins were estimated by Coomassie Blue staining of SDS-PAGE gels, with various amounts of bovine serum albumin protein used as standards. Mouse CLU cDNA fragments encoding amino acid residues 18–448 and 345–380 were amplified by PCR and inserted into the pT7Blue-2 vector (Novagen, Inc., Madison, WI) using the Perfectly Blunt™ Cloning kit (Novagen, Inc., Madison, WI) according to manufacturer's instructions. All cDNA expression vectors were sequenced to confirm cloning before use.

The TnT-coupled wheat germ extract system (Promega, Madison, WI) was used to generate S·Tag-fused, ^{35}S-labeled CLU protein fragments *in vitro* according to manufacturer's protocols. The amount of ^{35}S-labeled protein was estimated using the S·Tag Rapid Assay kit (Novagen Inc., Madison, WI), and an equal amount of transcription/translation mixture (40 μl) was added to glutathione-containing beads at the same molar amounts (0.2 pmol of CLU to 0.2 pmol of GST or GST-Ku70) and incubated overnight at room temperature. The mixture was then incubated at 4, 23, or 37 °C for 1 h, and beads were collected by centrifugation (15,000 × *g*), washed three times with ice-cold Binding buffer, resuspended in Laemmli buffer, and boiled, and proteins were resolved by 10–15% SDS-PAGE. ^{35}S-Labeled nCLU fragments were then visualized by autoradiography as described (33).

Intracellular Trafficking of nCLU and Mutant nCLU Proteins—To study the intracellular targeting of various nCLU fragments, we transfected MCF-7 cells with GFP-nCLU and GFP-nCLU deletion mutants. Effectin reagent (Qiagen Inc., Valencia, CA) was used to transfect 2 × 10^4 log phase MCF-7 cells that were pre-attached for 24 h to coverslips. Forty eight hours (48 h) later, cells were fixed for 1 h in freshly prepared 2% paraformaldehyde at room temperature. Cells were then rinsed twice in phosphate-buffered saline and treated with RNase A in phosphate-buffered saline (1 μg/ml) for 20 min at 37 °C. Cells were mounted in propidium iodide-containing Vectashield mounting media (Vector Laboratories Inc., Burlingame, CA) and subjected to confocal microscopy using a Bio-Rad MRC 1024 Confocal Laser Scanning microscope (Bio-Rad). All photomicrographs show representative z-sections at ×1000 magnification. At least 180 transfected cells (green) were visually screened for distribution of GFP-CLU protein in the cell and its co-localization with propidium iodide-stained nuclei (red). The number of cells with pycnotic propidium iodide *versus* normal nuclear morphology was manually counted, and percentages of apoptotic cells ± S.E. were calculated (see Table I). Likewise, the number of cells with nuclear only, cytoplasmic and nuclear, or cytoplasmic only localization of the GFP-fused proteins was manually counted. Percentages of cells with nuclear (or cytoplasmic and nuclear) or cytoplasmic only expression ± S.E. were calculated (Table II).

RESULTS

Identification of an nCLU-specific mRNA Splice Variant—After examining exon/intron sequences of the human *CLU* gene, we noticed an acceptor splice site two nucleotides upstream from the second in-frame AUG (codon 34) sequence of pnCLU (Figs. 1 and 2*A*). Located within exon III, this AUG codon was proposed to be the start site for the intracellular pnCLU protein (13, 22). In contrast to previous alternative

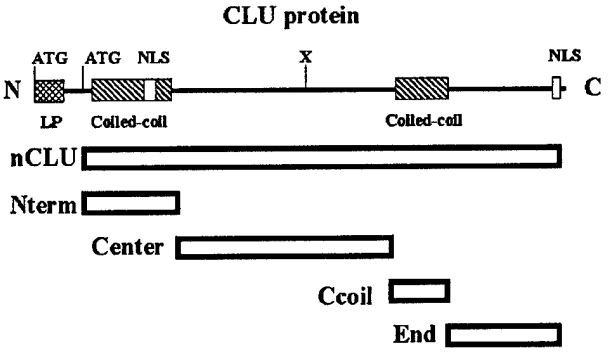

FIG. 1. **Structural map of the human CLU protein.** *Letters* and *boxes* signify the following: *LP*, endoplasmic reticulum-targeting hydrophobic leader peptide; *NLS*, nuclear localization signal; *X*, α/β-cleavage site (aa 205) of cytoplasmic ~60-kDa pre-secreted clusterin (psCLU); *slashed boxes* represent N- and C-terminal coiled-coil leucine zipper-like regions, aa 42–98 and 319–349, respectively. *Rectangles*, *nCLU*, *Nterm*, *Center*, *Ccoil*, and *End* signify the regions of CLU used for the generation of GFP-fused constructs (see Table I and Fig. 7).

translation start theories, we hypothesized that nCLU could be translated from low abundance mRNA produced by an alternative splicing event when exons I and III are spliced together. In this case, exon II that contained the first AUG and the ER-targeting signal of sCLU would be omitted. To verify this hypothesis, we used specifically designed primers, hCLU5′ to exon I and hCLUN-term-rev to exon IV (see "Experimental Procedures"), to amplify the 5′ ends of various splice variants of CLU cDNA derived from total RNA extracted from MCF-7 cells. The resulting RT-PCR fragments are shown in Fig. 2*B*. All visible fragments were excised from the agarose gel and sequenced. As expected, the 345-bp major fragment was identical in sequence to the 5′ end of sCLU. Two minor fragments with sizes of 450 and 550 bp had additional exons in the 5′-untranslated region and, therefore, did not contain any alterations in the open reading frame. Sequencing of the 220-bp fragment demonstrated, as we predicted for nCLU mRNA, the lack of exon II and direct junction between exons I and III (see Fig. 2*C*, *sequence*).

By using the primer to the 3′ end of the CLU open reading frame, we amplified full-length nCLU cDNA from MCF-7 cells. Sequence analyses confirmed the expected alternatively spliced full-length nCLU mRNA. No additional changes in the downstream exon composition of the nCLU cDNA were found.[3] Based on the data above, we concluded that human nCLU protein was translated from a separate, minor species of mRNA lacking exon II as a result of an alternative splicing event.

Identification and Analyses of Potential Functional Domains in nCLU—Analyses of the proposed primary aa composition of human and mouse CLU proteins, based upon respective CLU mRNA sequences, revealed two potential coiled-coil domains (Fig. 1). One coiled-coil domain was located in the N terminus (aa residues 42–98 in human and 42–97 in mouse) of nCLU, and the other coiled-coil domain was located in the C-terminal portion of both human and mouse nCLU proteins (residues 319–349 in human and 318–366 in mouse). Both C- and N-terminal domains appeared to be highly conserved and corresponded to "myosin-like" domains I and IV, identified previously by Tsuruta *et al.* (24). Both N- and C-terminal coiled-coil domains of CLU were rich in leucines and charged aa residues. We compared the characteristic 4-3 repeats of known coiled-coil domain-containing proteins GCN4, c-Jun, c-Fos, and BZLF1 (34-38) to the N- and C-terminal coiled-coil domains of human

[3] K. S. Leskov and D. A. Boothman, unpublished observations.

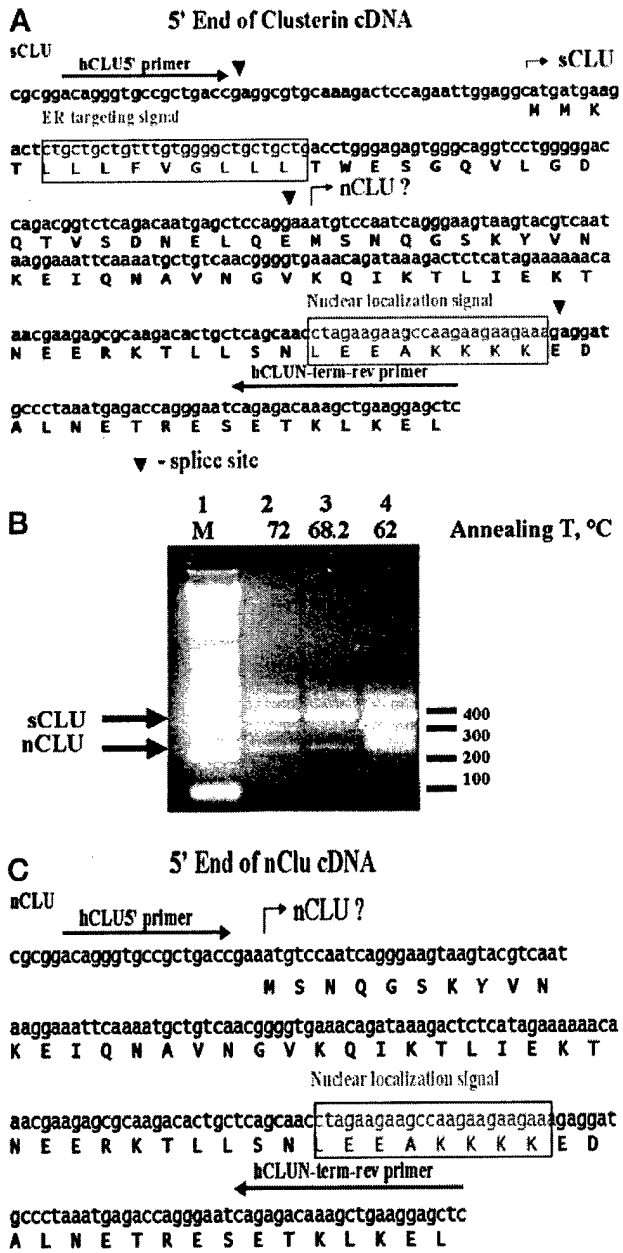

FIG. 2. *A*, two potential translation start sites of nCLU are located in the different exons. Structure of the 5′ end of sCLU cDNA is shown. Splice sites are indicated as *black triangles*. *Small arrows* show translational start sites of sCLU and nCLU. Endoplasmic reticulum targeting leader peptide (ER-targeting signal) and nuclear location signal are shown in *boxes*. *Long arrows* indicate primers used to amplify various spicing variants of CLU cDNA. *B*, alternative splicing of the 5′ end of CLU mRNA as detected by RT-PCR. PCR reaction was performed using hCLU5′ and hCLU-Nterm-rev primers (see *A*). Annealing temperatures were 72, 68.2, and 62 °C (*lanes 2–4*, respectively). *M* (*lane 1*), DNA marker. Note the position of nCLU (220 bp) and sCLU (340 bp) products. *C*, 5′ end of nCLU cDNA. Sequence of the 5′ end of nCLU cDNA that is the result of an alternative splicing event when exon II is omitted.

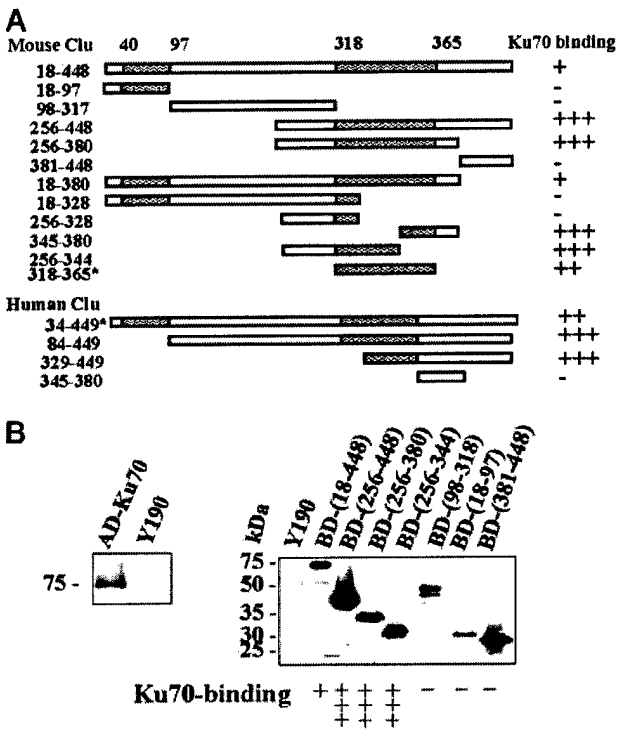

FIG. 3. *A*, the C-terminal coiled-coil domain of nCLU mediates Ku70 binding. The relative strength of nCLU-Ku70 interaction for both human and mouse pairs of proteins using yeast two-hybrid analyses are indicated as follows: +++, strong binding, colonies turned blue within 30 min of incubation with X-gal; ++, moderate binding, yeast colonies turned blue within 60 min; +, weak interaction, colonies turned blue within 120 min; −, no interaction, no blue colonies within 120 min of incubation with X-gal. nCLU constructs marked with *asterisks* were tested using yeast two-hybrid assays with GFP moieties on their N-terminal ends. The fusion of GFP to these proteins does not affect their cell death functions (13). Coiled-coil domains are shown as *slashed boxes*. *Numbers* represent the respective aa residues. Experiments were performed three or more times. *B*, expression of GAL4-fused proteins in Y190 yeast. Representative Western blot analyses of the expression of mouse Ku70 protein (*left panel*) used in two-hybrid analyses shown in *A* and GAL4AD- and GAL4BD-fused mouse nCLU deletion mutants (*right panel*) in Y190 yeast. *Plus signs* indicate binding of the particular nCLU fragment to mouse Ku70 as described in *A*.

and mouse nCLU (Fig. 4*A*). The C-terminal coiled-coil domain of nCLU contains a 4-3 repeat of predominantly hydrophobic residues, much like the BZLF1 gene product of the Epstein-Barr virus (38). The C-terminal coiled-coil domain of nCLU did not, however, contain a classical leucine zipper heptad. The 4-3 pattern within the predicted N-terminal coiled-coil domain consisted of both hydrophobic and charged residues.

Sequence analyses also indicated that the N-terminal coiled-coil domain of nCLU contained an SV40 large T-antigen-like NLS, LEEAKKKK (residues 74–81 in human and 73–80 in mouse) (22). In addition, we identified two other potential NLSs. One NLS-like sequence was found only in human nCLU (RRELDESLQVAERLTRK, residues 324–340) and was similar to the bipartite NLS found in the *Xenopus* nucleoplasmin protein (39). This potential NLS was not found in rodent nCLU protein. The other potential NLS in nCLU, RKKHR (residues 442–446) in human and RRKSR (residues 442–446) in mouse, was located at the very C terminus of the nCLU protein. Because functional NLSs in nCLU have also not been elucidated, we examined the role of coiled-coil domains and NLS sites for the cell death function of the protein and for association with Ku70.

The C-terminal Coiled-coil Domain of nCLU Is Essential for Binding to Ku70—A number of deletion mutants of human and mouse nCLU were constructed and tested for Ku70 binding using yeast two-hybrid analyses (Fig. 3*A*). Only those mutants containing the C-terminal coiled-coil domain, or a portion of the domain, were capable of interacting with the Ku70 protein. nCLU polypeptides containing the N-terminal domain (residues 18–97), a central region (residues 98–317), or a C-termi-

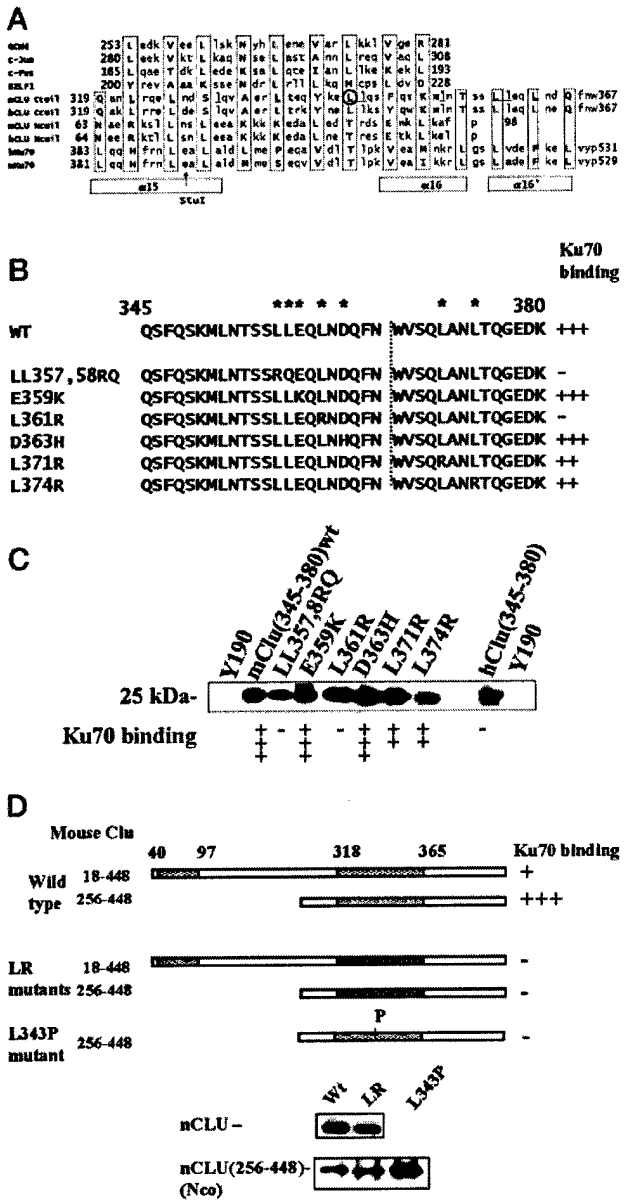

FIG. 4. *A*, the 4-3 repeats of hydrophobic residues within the protein-protein interaction domains of nCLU as compared with known coiled-coil domain-containing proteins. The 4-3 repeat-containing protein-protein interaction domains of GCN4, c-Jun, c-Fos, and BZLF1 are aligned according to Ref. 38 with predicted coiled-coil domains of human and mouse nCLU. The predicted C-terminal (*Ccoil*) and N-terminal (*Ncoil*) of human and mouse nCLU (*hCLU* and *mCLU*, respectively) are aligned with the potential nCLU-binding region of human and mouse Ku70 proteins (*hKu70* and *mKu70*, respectively). Every 1st, 3rd, and 4th residue is *capitalized* and *boxed*. Leucine residues in mCLU Ccoil that were targeted for the LR mutation are *underlined*. Leucine 343, which was targeted for the L343P mutation, is *circled*. *Rectangles* in the *bottom* indicate positions of α-helices 15, 16, and 16′ as noted (45). The *arrow* indicates the position of the *StuI* site, which was used to create a deletion that resulted in a Ku70 mutant protein unable to bind to nCLU (14). *Numbers* refer to the positions of the first and last residues within the full-length proteins. *B*, identification of aa residues of nCLU that mediate Ku70 binding. The relative strength of various mutant forms of mouse nCLU associating with mouse Ku70 were tested using yeast two-hybrid analyses as described in Fig. 3 and "Experimental Procedures." *Numbers* represent the respective aa residues of mouse nCLU protein. Amino acid residues targeted for mutations are marked with *asterisks*. Residues to the *left* of the *dotted line* are inside the predicted C-terminal coiled-coil domain of mouse nCLU. Residues to the *right* side of the *dotted line* are outside the functional C-terminal coiled-coil domain. Relative strength of binding was scored as described in Fig. 3*A*, and experiments were performed three or more times. *WT*, wild type. *C*, GAL4-fused mutants of nCLU-(345–380) fragments are expressed in Y190 yeast. Western blot analyses demonstrate expression of mouse nCLU point mutants within aa 345–380 and the corresponding human aa 345–380 nCLU fragment in Y190 yeast. The relative strength of Ku70 binding was described in Fig. 3*A*, and all experiments were performed three or more times. *D*, LR mutants (nCLU-LR and *Nco*LR) of mouse nCLU and mouse nCLU-(256–448) protein fragment and L343P mutant of mouse nCLU-(256–448) fragment do not bind to Ku70. Yeast two-hybrid analyses were performed to determine binding of wild-type, L343P, and LR mutants of mouse nCLU and nCLU 256–448 proteins to Ku70. Mouse nCLU fragment (aa 318–365) contains C-terminal coiled-coil domain, and wild-type, LR mutant, and L343P (*with a P*) nCLU proteins are also shown. The relative strength of binding of mouse nCLU LR mutants to mouse Ku70 protein was indicated as described in Fig. 3 and "Experimental Procedures." The experiments were performed three or more times. *E*, steady-state levels of nCLU wild-type, LR, and L343P mutant proteins are equal when expressed in the Y190 yeasts. The expression and stability of full-length mouse nCLU wild-type and nCLU-LR mutant (*top panel*), as well as nCLU fragment aa 256–448, *Nco*LR, and L343P mutants of the same fragment (*lower panel*) in Y190 cells were assessed by Western blot analyses using anti-GAL4BD antibody. Expression of proteins in all experiments described in *B* were confirmed by Western blotting.

nal fragment (residues 381–448) of the protein did not interact with Ku70. None of these nCLU fragments contained the C-terminal coiled-coil domain. Two nCLU polypeptides encompassing aa residues 256–344 and 345–380, respectively, contained only a portion of the C-terminal coiled-coil domain. Interestingly, these two nCLU fragments showed strong interaction with Ku70. Steady-state expression of GAL4-fused proteins, both Ku70-binding and non-binding polypeptides, are shown in Figs. 3*B* and 4*B*. These findings suggested that the C-terminal coiled-coil domain of nCLU was important for its interaction with Ku70. Furthermore, these data suggested that half, or less, of the coiled-coil domain was sufficient to bind Ku70 in yeast two-hybrid assays.

To study the role of specific residues in nCLU-Ku70 binding, we concentrated on the nCLU polypeptide fragment containing residues 345–380 (nCLU-(345–380)). This fragment displayed strong binding to Ku70 and contained only 22 residues of the predicted C-terminal coiled-coil domain. Because the Ku70-binding domain of nCLU contained a putative 4-3 hydrophobic repeat motif, we determined whether specific leucine repeat residues within nCLU-(345–380) were necessary and sufficient to mediate Ku70-nCLU binding. The following point mutations were introduced: (*a*) L357R,L358Q (a double substitution of leucines 357 and 358 to arginine and glutamine, respectively); (*b*) E359K; (*c*) L361R; (*d*) D363H; (*e*) L371R; and (*f*) L374R, L357R,L358Q, E359K, L361R, and D363H were point mutations made inside the nCLU coiled-coil domain, whereas L371R and L374R were substitutions made outside the coiled-coil domain (Fig. 4*B*). Substitution of leucine residues inside the coiled-coil domain structure of nCLU-(345–380) completely abrogated Ku70 binding. Substitutions of leucine residues outside the coiled-coil domain decreased the association of each nCLU-(345–380) peptide with Ku70 but did not completely abrogate protein-protein interaction. Mutations of two non-leucine residues that were not part of the 4-3 repeat within the same region of the protein (E359K and D363H) did not affect nCLU-(345–380) binding to Ku70. These data strongly suggested that only residues that constituted the 4-3 hydrophobic repeat inside the C-terminal coiled-coil domain of nCLU mediated its interaction with Ku70. Leucines 371 and 374 immediately outside the coiled-coil domain of nCLU may, therefore, stabilize protein-protein interaction but do not appear to be essential for Ku70 binding.

Additional evidence suggesting the importance of the coiled-coil structure of nCLU and its interaction with Ku70 came from

deletion analyses using human nCLU cDNA/protein and human Ku70 as bait in yeast two-hybrid analyses (Fig. 3*A*). Our limited analyses suggest that aa residues 326–365 are minimally essential for the association of nCLU with Ku70. The human homolog portion of the mouse nCLU-(345–380) polypeptide fragment was unable to bind human Ku70 (Fig. 3*A*). This fragment of human nCLU contained leucines in positions 357, 358, and 361 that were essential for mouse nCLU binding to Ku70. However, the predicted C-terminal coiled-coil domain of human nCLU was shorter than in mouse nCLU. This shortened length of the C-terminal coiled-coil domain of human nCLU was apparently due to the presence of a tryptophan residue at position 350 in human nCLU that presumably interferes with α-helical secondary structure. Thus, human nCLU appears to have a more tightly compact Ku70 interaction domain than the comparable domain present in the mouse protein.

To confirm the role of hydrophobic residues in the context of full-length nCLU for Ku70 binding, we created mouse nCLU mutants (designated as LR mutants) with nine leucine residues within the C-terminal coiled-coil domain substituted by arginines as described under "Experimental Procedures." Leucines 326, 330, 336, 343, 344, 352, 357, 358, and 361 were mutated to arginines (LR mutant) in the full-length nCLU (nCLU-LR), nCLU-(256–448) (*Nco*LR), as well as nCLU-(218–365) (CcLR). NCLU-LR and *Nco*LR mutants were tested by yeast two-hybrid analyses for Ku70 binding, along with their wild-type counterparts. Both NCLU-LR and *Nco*LR mutants were unable to bind mouse Ku70 protein (Fig. 4*D*) under conditions where each mutant protein was expressed in transformed yeast cells (Fig. 4*E*). In contrast, their wild-type counterparts (nCLU and nCLU 256–448) strongly associated with Ku70.

To investigate the role of the α-helical structure of the C-terminal coiled-coil domain in Ku70 binding, we introduced a single proline residue at position 343 (L343P mutant) in the context of the nCLU aa 256–448 C-terminal half of the protein. When tested by yeast two-hybrid analyses, this mutant did not show detectable binding to Ku70. Equal expression of wild-type and L343P mutant proteins in yeast was confirmed by Western blot analyses (Fig. 4*E*).

GST-Ku70 Pull-down Analyses Confirm Yeast Two-hybrid Results—To confirm the yeast two-hybrid data, we utilized GST-Ku70 *in vitro* binding (pull-down) assays. GST-Ku70 and GST proteins were expressed in bacteria and immobilized on glutathione-Sepharose beads as described under "Experimental Procedures" (Fig. 5*B*). ^{35}S-Labeled mouse nCLU polypeptide was used to determine optimal Ku70-binding conditions (Fig. 5*A*). Minimal nCLU binding to GST was detected in a temperature-insensitive fashion as described by Humphreys *et al.* (20). Significant interaction of nCLU with GST-Ku70 was detected when incubation temperatures were between 23 and 37 °C, whereas nCLU binding to an equal amount of GST alone did not change with temperature (Fig. 5*A*). At 4 °C, nCLU binding to GST-Ku70 was not significantly higher than background. These data indicated a temperature-dependent association of nCLU binding to Ku70, and that a temperature-sensitive conformational change was necessary for protein-protein association.

Point mutations in mouse nCLU fragment 345–380 at L357R,L358Q, E359K, L361R, D363H, and L371R were then examined using GST-Ku70 *in vitro* binding assays (Fig. 5*C*). The results were identical to those obtained by yeast two-hybrid analyses, except that mutant E359K showed unexpectedly high binding to GST-Ku70 compared with wild-type nCLU, suggesting that some non-4-3 repeat residues inside the coiled-coil domain might also modulate Ku70 binding.

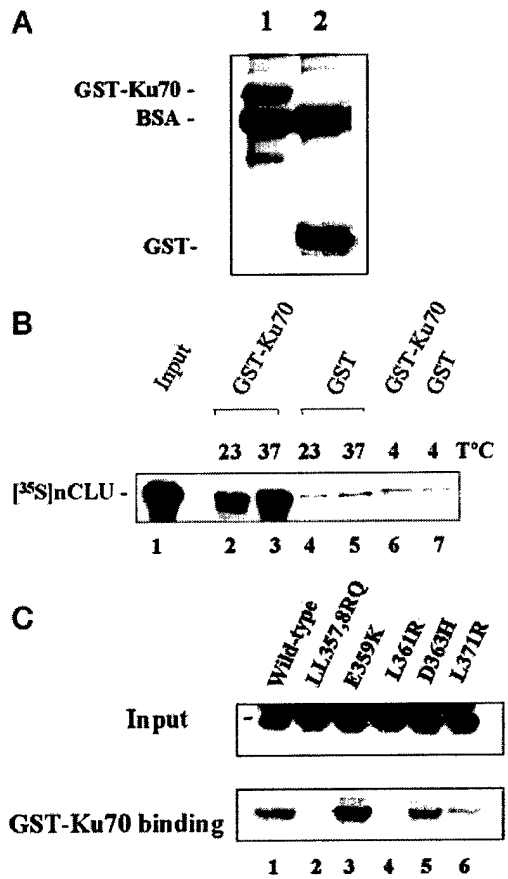

FIG. 5. *A*, relative amounts of agarose-immobilized proteins used in the GST-pull-down assays. To estimate the amount of GST and GST-Ku70 proteins used in the *in vitro* nCLU-binding assay, glutathione-agarose beads with immobilized proteins (20 μl of 50% suspension) were heated in the presence of equal amounts of 2× Laemmli buffer and resolved on the 10% acrylamide SDS-PAGE followed by Coomassie Blue staining. *Lane 1*, GST-Ku70 agarose beads; *lane 2*, GST alone agarose beads. Bovine serum albumin (*BSA*) was used as a blocking reagent and was present in both samples. *B*, nCLU binds GST-Ku70 *in vitro*. Autoradiograph of *in vitro* binding of mouse nCLU (aa 18–448) to GST-fused full-length mouse Ku70 protein and to GST as analyzed by 10% SDS-PAGE as described under "Experimental Procedures." The lanes from *left* to *right* are as follows: *1*, input protein, 5 μl of the nCLU *in vitro* translation reaction mixture; *2*, *in vitro* translated nCLU (from 45 μl of translation mixture) eluted from GST-Ku70-agarose beads, incubation temperature 23 °C; *3*, same as in *lane 2*, with an incubation temperature of 37 °C; *4*, *in vitro* translated ^{35}S-nCLU (from 45 μl of translation mixture) eluted from the GST-agarose beads, incubation temperature 23 °C; *5*, same as in *lane 4*, with an incubation temperature of 37 °C; *6*, eluted from GST-Ku70-agarose beads, with an incubation temperature of 4 °C; *7*, eluted from GST-agarose beads, with an incubation temperature of 4 °C. *C*, leucine residues within the C-terminal coiled-coil domain of nCLU are necessary for GST-Ku70 binding *in vitro*. Autoradiograph of the SDS-PAGE (15% acrylamide) representing *in vitro* binding of mouse nCLU aa 345–380 to GST-fused full-length mouse Ku70 protein. To confirm the results of yeast two-hybrid analyses of Ku70 binding to various nCLU point mutants, the same mutants of mouse nCLU aa 345–380 fragment were translated *in vitro* and tested for their ability to interact with GST-Ku70. *Top panel* shows the relative input amounts of *in vitro* translated wild-type and point mutants of the mouse nCLU fragment (5 μl of each reaction mixture). *Bottom panel* shows GST-Ku70 binding to the respective mouse nCLU protein fragments retained on the GST-Ku70-agarose beads. 45 μl of each reaction mixture were used for the binding assay as described previously (32). The *lanes* from *left* to *right* are as follows: *1*, wild-type nCLU aa 345–380 fragment; *2*, LL357,8RQ mutant; *3*, E359K mutant; *4*, L361R mutant; *5*, D363H mutant; and *6*, L371R mutant.

The Coiled-coil Domains of nCLU Bind Each Other—The longest Ku70-binding nCLU polypeptide (residues 84–449),

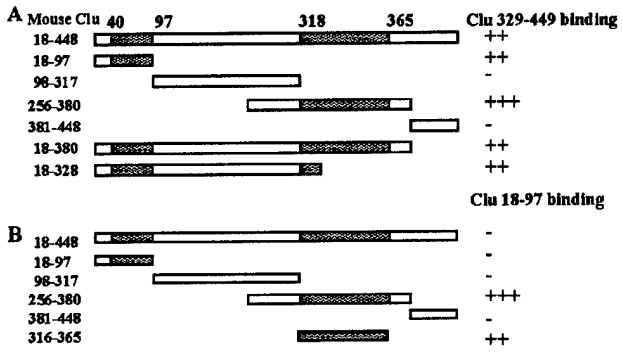

FIG. 6. **N- and C-terminal coiled-coil domains bind to each other in yeast two-hybrid system.** The human nCLU deletion mutant containing aa 329–449 (*A*) or the mouse nCLU deletion mutant containing aa 18–97 (*B*) coiled-coil domains were used as bait to analyze their abilities to bind to various deletion mutants of mouse nCLU. *Numbers* represent corresponding amino acid residues. The potential coiled-coil regions are illustrated as *shaded boxes*. Relative strength of protein-protein binding (*plus signs*) was indicated as described in Fig. 3*A*, and all experiments were performed three or more times.

isolated from the human liver cDNA library by yeast two-hybrid screening, excluded most of the N-terminal coiled-coil domain (14). However, all nCLU polypeptides that interacted with Ku70 contained the C-terminal coiled-coil domain. Interestingly, full-length nCLU cDNA containing C- and N-terminal coiled-coil domains was not isolated in the initial yeast two-hybrid screen (14). The reasons for the absence of full-length nCLU were unclear. One possible explanation for the lack of isolation of full-length nCLU cDNA was that the N-terminal coiled-coil domain might bind to the C-terminal coiled-coil domain of nCLU and interfere with Ku70 binding (see below). Yeast two-hybrid analyses of a number of nCLU deletion mutants showed that whenever two coiled-coil domains of nCLU were present in the same molecule (*e.g.* polypeptides containing aa residues 18–380 of mouse nCLU and human nCLU fragment containing aa residues 34–449), binding of these fragments to Ku70 was notably lower compared with nCLU polypeptides containing a single C-terminal coiled-coil domain (*i.e.* see mouse nCLU mutants containing residues 256–448, and the human nCLU polypeptide fragment containing residues 84–449) (Fig. 3*A*). These data suggested to us that the N-terminal coiled-coil domain of nCLU might compete with Ku70 for binding to the C-terminal coiled-coil domain of nCLU.

Because the N-terminal coiled-coil domain of nCLU did not interact with Ku70 (Fig. 3*A*), we hypothesized that this N-terminal domain of nCLU might act as a suppressor of nCLU-Ku70 protein-protein interaction. Therefore, we examined the ability of coiled-coil domains of nCLU to bind each other. The C-terminal coiled-coil domain of human nCLU (*i.e.* a fragment containing aa residues 329–449) was used as "bait." The C-terminal coiled-coil domain of nCLU was also able to interact with the N-terminal domain of the protein (aa 18–97) and with itself (aa 256–380) (Fig. 6*A*). However, neither the central portion of nCLU (aa 98–317) nor a C-terminal fragment of nCLU missing the coiled-coil domain (aa 381–448) interacted with either the C- or N-terminal coiled-coil domains of nCLU. In addition, when tested as bait, the N-terminal coiled-coil domain interacted only with the C-terminal coiled-coil domain (Fig. 6*B*). The N-terminal coiled-coil domain did not interact with itself nor with central or C-terminal fragments of nCLU that lacked coiled-coil structures. These data strongly support the theory that the coiled-coil domains of nCLU may indeed be involved in either intra- or intermolecular interactions.

Intracellular Targeting of nCLU Domains and Induction of Apoptosis by Specific nCLU Proteins—Previous analyses of the nCLU aa sequence identified one NLS within its N-terminal coiled-coil domain (40) and another within the C-terminal fragment, but outside its coiled-coil domain (13). To investigate the role of these NLSs in the subcellular localization of the nCLU protein and in the cell death functions of the protein, we transfected MCF-7 breast cancer cells with GFP-fused constructs of wild-type and NLS mutants of the nCLU protein (used above). MCF-7 cells were chosen because we characterized previously (13) nCLU translocation in these cells following IR. Confocal microscopic analyses of the subcellular localization of various GFP-CLU fragments in MCF-7 cells 48 h post-transfection were then noted (Fig. 7), and the percentage of apoptosis ± S.E. was quantified (Table I). Surprisingly, exogenously overexpressed full-length GFP-nCLU fusion protein was mostly cytosolic with minor expression noted in the nuclei of some transfected (*green*) cells (Fig. 7, *B* and *C*). In fact, the GFP-nCLU-positive population could be divided into two types. One population contained cells with normal nuclear morphology and very bright GFP-nCLU aggregates in the cytosol and perinuclear space (Fig. 7*C*), similar to untreated MCF-7 cells stained for endogenous nCLU protein (13). These aggregates did not co-localize with the ER, the Golgi apparatus, or mitochondria when co-stained with the following organelle-specific fluorescent markers: Texas Red-conjugated concanavalin A, Texas Red X-conjugated wheat germ agglutinin), and MitoTracker Red (Molecular Probes, Eugene, OR). Virtually no GFP-nCLU was detected in nuclei of cells within this subpopulation of transfectants, and virtually none of these cells showed classical apoptotic morphology. Another subpopulation of GFP-nCLU transfectants (~15% of GFP-nCLU-positive cells as determined by visual screening) had diffuse distribution of GFP-nCLU with some apparent GFP-nCLU expression in nuclei (Fig. 7*B*). Most importantly, all cells that had visible nuclear GFP-nCLU expression had condensed chromatin, characteristic of apoptotic cells (41). Expression of GFP-Nterm protein in MCF-7 cells was diffusely distributed and located in both the cytosol and nucleus of transfected cells (Fig. 7*D*). In contrast, expression of the GFP-Center fusion protein within MCF-7 cells resulted in the formation of cytosolic aggregates (Fig. 7*E*), similar to the pattern of protein expression observed in the non-apoptotic subpopulation of the GFP-nCLU MCF-7 transfectants, as well as to the endogenous nCLU expression pattern in non-irradiated MCF-7 cells (13). Few, if any, GFP-Center-transfected MCF-7 cells exhibited apoptosis or any other abnormal morphology. These data strongly suggested that the apoptotic effects of nCLU are specific and that cytosolic localization and aggregate formation are attributed to protein regions separate from the domain responsible for nCLU-induced cell death. In contrast, the distribution of GFP-Ccoil (Fig. 7*F*) protein in both cytosol and nucleus resembled the subpopulation of apoptotic cells transfected with GFP-nCLU (Fig. 7*B*). As with GFP-nCLU, the presence of apoptotic nuclei following GFP-Ccoil transfection coincided with GFP-positive nuclear staining, and few apoptotic, non-transfected cells were noted within the transient cell population. No GFP-positive cells with large aggregates were detected in the GFP-Ccoil transfectants, as observed in the non-apoptotic GFP-positive subpopulation present within 48 h following GFP-nCLU transfection (Fig. 7*C*). Transfection of MCF-7 cells with GFP-End (that lacks a coiled-coil domain but has a C-terminal NLS) resulted in very few cells with large aggregates in their cytoplasm, and the majority of protein was expressed in the nuclei of GFP-positive MCF-7 cells (Fig. 7*G*). Unlike transfection with GFP-nCLU (Fig. 7*B* and Table I), few cells with apoptotic morphology were detected among the GFP-End transfectants. A single L343P mutation within the C-terminal coiled-coil domain of GFP-

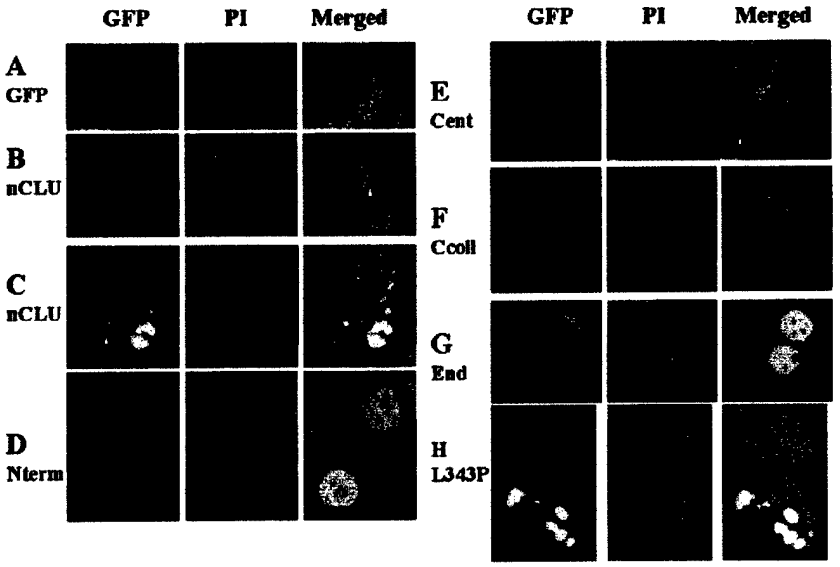

FIG. 7. **Subcellular localization of various GFP-fused nCLU fragments in MCF-7 cells.** MCF-7:WS8 cells were transfected with various GFP-fused mouse nCLU fragments, and transfectants were analyzed 48 h post-transfection using confocal microscopy for protein localization and cell death responses. Images in each row display the following: *left* (*GFP*), GFP-fused nCLU protein; *middle* (*PI*), propidium iodide (*PI*)-stained DNA; *right* (*Merged*), digitally merged *green* and *red* images; therefore, *yellow* demonstrates co-localization. *Rows* are defined as follows: *A*, GFP alone; *B* and *C*, GFP-nCLU; *D*, GFP-Nterm; *E*, GFP-Center; *F*, GFP-Ccoil; *G*, GFP-End; and *H*, GFP-nCLU L343P mutant. Note the diffuse expression of GFP-nCLU fused proteins in transfections *A*, *B*, *D*, *F*, and *G*. Note the punctated appearance of GFP-nCLU (*C*), GFP-Center (*E*), and GFP-nCLU L343P mutant (*H*) following transfection in MCF-7 cells, and the appearance of two subpopulation with diffuse or aggregated protein expression following GFP-nCLU transfection in MCF-7 cells. Also note nuclear localization of GFP-Nterm and GFP-End. See Table I for quantitation of apoptotic responses.

TABLE I

Induction of apoptosis by exogenously expressed GFP-fused nCLU protein fragments

Log phase MCF-7 cells were transfected with either GFP- or GFP-nCLU-fused cDNAs and analyzed 48 h later by confocal microscopy. z-sections were then analyzed for protein localization (Fig. 7), and percentages of apoptotic cells among GFP-positive cells were quantified. Apoptotic cells were defined as cells with condensed and fragmented pycnotic nuclei (Fig. 7). Values are mean ± S.E., representing three independent transient transfections. At least 200 GFP-positive cells were counted for each GFP construct per experiment.

Protein expressed	Cells with pycnotic nuclei (% of total) ± S.E.
GFP	4 ± 1
GFP-nCLU	25 ± 5
GFP-N-term	5 ± 12
GFP-Center	5 ± 1
GFP-Ccoil	31 ± 4
GFP-End	2 ± 0.5
GFP-nCLU L343P	2 ± 0.3

nCLU (Fig. 7*H*, Table I) resulted in little or no detectable cell death and punctated cytoplasmic localization of the GFP-nCLU L343P protein. Transfection of MCF-7 cells with vector expressing GFP alone resulted in cells with diffusely distributed protein expression, mostly in the cytoplasm of transfected cells (Fig. 7*A*). Few apoptotic or other abnormal morphologies were noted in GFP-positive expressing MCF-7 cells after transfection with GFP alone, as found with GFP-Nterm, GFP-Center, and GFP-End (Fig. 7, *D*, *E*, and *G* and Table I).

nCLU Protein Has Two Functional NLS Motifs—It was proposed previously (13, 22) that the nCLU protein contains two conserved potential NLSs among species. We define the N-terminal NLS as NLS1 and C-terminal as NLS2. To identify the functional NLS of nCLU, we introduced point mutations in the respective NLS sequences. We mutated NLS1, ^{77}KKKK^{80} to ^{77}KAVK^{80} in the context of mouse GFP-Nterm protein (NLS1mut), and NLS2, ^{442}RRKSR^{446} to ^{442}VVKSR^{446} in the context of mouse GFP-End protein (NLS2mut). The nCLU protein fragments were chosen because they elicited no apoptotic responses, which could influence the trafficking analyses. We transfected MCF-7 cells with NLS1mut, NLS2mut, GFP-Nterm wild-type, GFP-End wild-type or GFP alone, and we determined the intracellular localization of the GFP-fused protein 48 h post-transfection (Fig. 8). The percentage of cells with cytoplasmic *versus* nuclear localization of GFP-fused proteins are summarized in Table II. Although GFP-alone control cells expressed GFP predominantly in the cytoplasm (Fig. 8*A*), we noticed uniform distribution of the wild-type GFP-Nterm in 57 ± 5% cells with expression in both the cytoplasm and nucleus (Fig. 8*B*). Mutation in the N-terminal NLS led to an ~2.5–3-fold decrease in percentage of cells with detectable nuclear expression of GFP-Nterm NLS1mut (Fig. 8*C*, Table II). As in Fig. 7*G*, localization of GFP-End was predominantly nuclear (98 ± 0.2% cells with nuclear expression, Fig. 8*D*). In contrast, GFP-End NLS2mut was detected only in the cytoplasm in 78 ± 5% of GFP-positive cells (Fig. 8*E*). Based on these data, we conclude that both NLS1 and NLS2 of nCLU are functional; however, NLS2 is a relatively stronger site, resulting in greater differences in nuclear localization of GFP-End *versus* GFP-End NLS2mut.

DISCUSSION

The exact role(s) of alterations in CLU gene expression before and after cytotoxic stress remain(s) a mystery. Our data indicate that human cells synthesize CLU protein forms that lack ER-signaling peptides and are destined for functions in the cytoplasm and nucleus. This is in contrast to the sCLUs that are currently thought to exert cytoprotective effects on exposed cells as well as effects on non-damaged bystander cells as discussed previously (42, 43). Collectively, our data suggest that nCLU contributes to cell death. Previous data (13, 22) indicated the existence of a mature ~55-kDa nCLU protein. The nCLU protein did not appear to be either glycosylated or cleaved at its α/β-site, a site cleaved during maturation of the 60-kDa sCLU precursor protein. nCLU was induced by rela-

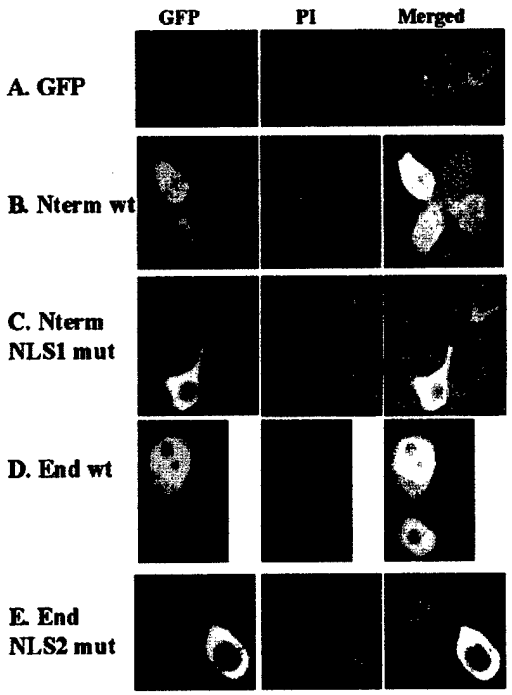

FIG. 8. **nCLU has two functional NLS motifs.** MCF-7 cells were transfected with GFP-fused mouse Nterm or End fragments, with or without mutations in the N-terminal and C-terminal NLSs, respectively. Transfectants were examined 48 h post-transfection using confocal microscopy. Images in each row display the following: *left* (*GFP*), GFP-fused nCLU protein; *middle* (*PI*), propidium iodide (*PI*)-stained DNA; *right* (*Merged*), digitally merged *green* and *red* images; therefore, *yellow* demonstrates co-localization. Rows are defined as follows: *A*, GFP alone; *B*, GFP-Nterm wild type; *C*, GFP-Nterm N-terminal NLS mutant; *D*, GFP-End wild type; *E*, GFP-End C-terminal NLS mutant. See Table II for quantitation of the percentage of the cells with nuclear *versus* cytoplasmic localizations of GFP-fused proteins.

TABLE II
Mutations in NLS1 or NLS2 result in cytoplasmic localization of GFP-nCLU constructs

Log phase MCF-7 cells were transfected with either GFP- or GFP-nCLU-fused cDNAs with or without mutations in NLS1 and NLS2, as described in the text, and analyzed 48 h later by confocal microscopy. z-sections were then analyzed for protein localization (Fig. 8), and the percentages of cells with cytoplasmic or cytoplasmic and nuclear localization of GFP-fused proteins were quantified. The numbers with standard errors are the result of three independent transient transfections. At least 200 GFP-positive cells were counted for each GFP construct per experiment.

Protein expressed	% localization ± S.E.	
	Cytoplasm	Nucleus (nucleus and cytoplasm)
GFP-Nterm wild-type	43 ± 5	57 ± 5
GFP-Nterm NLS1 mutant	79 ± 3	21 ± 3 (2-fold)
GFP-End wild-type	2 ± 0.2	98 ± 0.2 (2-fold)
GFP-End NLS2 mutant	78 ± 5	22 ± 5
GFP	88 ± 2	12 ± 2

tively high levels of cytotoxic stress (*e.g.* IR) in direct proportion to lethality, compared with sCLU protein increases that were very sensitive to low, nontoxic, and growth stimulatory doses of IR (13). Utilization of a second downstream AUG start site was proposed to result in the synthesis of an ~49-kDa precursor nCLU protein that resided in the cytoplasm of undamaged cells by confocal microscopy (13). nCLU greatly accumulated and translocated to the nuclei of cells 48–72 h after IR exposure. Overexpression of nCLU, even without IR treatment, caused cell death (*i.e.* apoptosis). The mechanism of synthesis of this

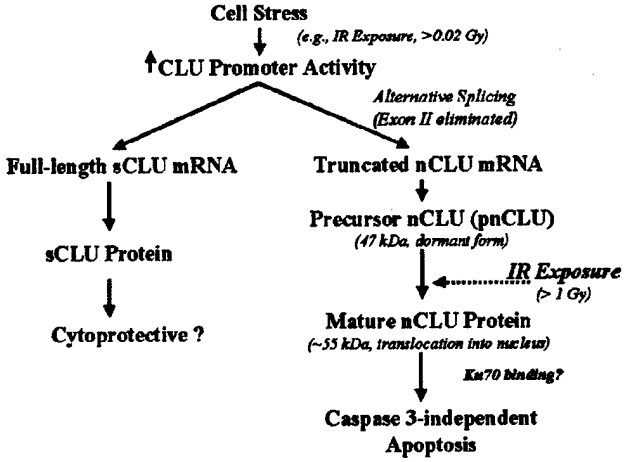

FIG. 9. **A model for nCLU synthesis in human epithelial cancer cells.** CLU promoter activity is stress-inducible (T. L. Criswell, D. A. Boothman, K. S. Leskov, and D. Y. Klokov, unpublished data). The precursor transcript of the CLU mRNA is spliced in various ways, producing the highly abundant sCLU mRNA (with exon II) and a much lower abundance pnCLU mRNA (without exon II). sCLU protein is targeted to the ER and secreted outside the cell. In contrast, the ~49-kDa pnCLU protein stays in the cytoplasm and can be modified following stress to produce mature 55-kDa nCLU protein when the radiation dose is equal or exceeds ~1 Gy (42). nCLU is imported into the nucleus where it binds Ku70 via its C-terminal coiled-coil domain. Overexpression of nCLU results in caspase-3-independent apoptosis (13). The C-terminal, Ku70-binding coiled-coil domain is required for the apoptotic function of nCLU.

nuclear protein from the second AUG translation start site, and how translation could bypass the much stronger first translation CCAUG start site present in full-length CLU mRNA, was not elucidated. Previous investigations did not address how the precursor ~49-kDa nCLU protein (pnCLU) might reside in the cytoplasm of undamaged cells in an apparent nonfunctional form (13), and then dramatically accumulate in the nuclei of damaged cells as an ~55-kDa mature nCLU death protein 48–72 h after exposure (13). Finally, no previous study attempted to elucidate the functional domains of the nCLU protein and, in particular, to identify the portions of the protein required for cell death, Ku70 binding, and/or nuclear localization. In fact, the need for nuclear localization in the cell death function of the protein was not established.

The data presented in this paper begin to address these processes and are consistent with the proposed hypothetical model of nCLU synthesis and cell death functions shown in Fig. 9, and discussed below. Our data show that a unique, shortened form of the nCLU mRNA is present at low levels (detected only by RT-PCR) in undamaged cells, and presumably increases after IR exposure in direct proportion to accumulation of full-length CLU mRNA. The low abundance, truncated form of the nCLU mRNA is the result of alternative splicing that eliminates exon II, including the first strong AUG start site. Translation from this truncated nCLU mRNA results in the production of an ~49-kDa nCLU precursor protein (*i.e.* pnCLU) that is initiated from a second downstream AUG translational start site (located in exon III), and the protein produced (pnCLU) lacks the ER signal peptide. The ~49-kDa pnCLU appears to contain at least two functional NLSs that targeted the protein to the nucleus. Only overexpression of nCLU proteins that have C-terminal coiled-coil domains and a functional NLS caused cell death. The nCLU protein has two coiled-coil domains, one at its N terminus that is unable to bind Ku70, and a C-terminal coiled-coil domain that is uniquely able to associate with Ku70 and is minimally required for cell death. The N-terminal coiled-coil domain of nCLU can associate with the C-terminal coiled-

coil domain of the nCLU protein. Specific mutations in, or deletions of, the C-terminal coiled-coil domain of nCLU simultaneously abrogated Ku70 binding and prevented cell death, even though these mutant forms of the nCLU protein accumulated in the nuclei of transfected MCF-7 cells (Fig. 7). Our data further support a role of Ku70 binding in the cell death function of mature nCLU. We show that only nCLU proteins containing both the C-terminal coiled-coil domain and a functional NLS can kill MCF-7 cells after transfection. Alterations in, or deletions of, the C-terminal NLS or C-terminal coiled-coil domain abrogated cell death. However, attempts to date to show conclusively that Ku70 is necessary for cell death caused by nCLU have yielded inconclusive results due largely to the enhanced apoptotic indices of $Ku70^{-/-}$ cells, observed with SV40-transformed murine embryonic fibroblasts (44). The generation of mutant nCLU proteins with alterations in the C-terminal coiled-coil domain or NLS should allow us to elucidate the role of nCLU-Ku70 binding in the cell death functions of nCLU in the future.

Synthesis of nCLU—Our data show that a low abundance nCLU mRNA is constitutively made in MCF-7 cells, in direct proportion (but in low abundance) to total CLU mRNA. Translation from this nCLU mRNA produces an ~49-kDa nCLU precursor protein (Fig. 9, *pnCLU*). Detection of this truncated nCLU mRNA in human cells argues against the more unlikely production of the ~49-kDa pnCLU through internal ribosome entry site-mediated translational initiation from a second in-frame AUG sequence in full-length CLU mRNA as suggested (13, 22). There is precedence for alterations in the subcellular localization of protein species via alternative splicing, as proposed for nCLU (Fig. 9). Expression of the rat renin protein undergoes alternative splicing, producing either secreted or intracellular forms of the protein from two unique mRNAs (42). We are investigating the mechanisms of alternative splicing of the CLU mRNA. In particular, we are examining the possible inducibility of nCLU-specific splicing events in response to IR or other cellular stresses. Previous data showed that mature ~55-kDa nCLU protein could be modestly induced (~2-fold) following 1 Gy of IR, compared with more dramatic >50-fold increases in sCLU protein forms. We propose that this reflects the relative abundance of the two mRNA species. Because the truncated, alternatively spliced form of nCLU mRNA was apparent in undamaged cells, our data suggest that the ~49-kDa precursor nCLU protein is constitutively synthesized in cells and stored in a reservoir. The stored protein can then be activated by an as yet unidentified post-translational modification after certain threshold doses of IR (>1 Gy), resulting in an ~55-kDa mature nCLU protein (Fig. 9). Such a mechanism would explain expression of the protein without triggering cell death responses. Localization of pnCLU in the cytoplasm of non-treated cells by confocal microscopy, with no detectable levels in the nuclei of untreated MCF-7 cells (13), appears to support a possible mechanism of sequestration of the pnCLU protein to prevent cytotoxicity.

Functional Domains of the nCLU Protein—Our data strongly suggest that nCLU-Ku70 binding was facilitated by strong leucine zipper-like hydrophobic interactions, mediated by the C-terminal coiled-coil domain in nCLU and a comparable coiled-coil domain in Ku70. Deletion of more than one hydrophobic residue in the full-length C-terminal coiled-coil domain of nCLU was not sufficient to abrogate nCLU-Ku70 binding (Fig. 3*A*, deletion mutants *256–344* and *345–380*), apparently due to redundancy of hydrophobic residues required for association with this protein. Introduction of a single proline residue that was inconsistent with the α-helical coiled-coil domain (L343P mutation) completely abrogated Ku70 binding (Fig. 4*D*) and cell death (Fig. 7*H*). Thus, the coiled-coil domain is absolutely required for interaction with Ku70 and initiation of cell death. It is important to note that the overall length of the C-terminal coiled-coil domain of nCLU is almost twice as large as the dimerization domains of GCN4, c-Fos, c-Jun, and BZLF1. This could explain our finding that deletion of a significant portion of the C-terminal coiled-coil domain of nCLU did not affect protein-protein interaction.

Our previous studies showed that in-frame deletion of aa residues 492–583 of Ku70 abrogated nCLU-Ku70 binding. Recent structural data on the Ku complex (43) indicated that this deletion affected α-helices 15, 16, and 16′ that also contained 4-3 patterns of hydrophobic amino acids (Fig. 4*A*). The ultimate role of the 4-3 repeated hydrophobic residues in mediating Ku70 binding was elucidated using point mutation analyses of the 345–380 minimal Ku70-interacting fragment of nCLU. Thus, the interaction between Ku70 and nCLU appears to occur through the C-terminal coiled-coil domain of nCLU, a region of the protein also required for cell death (only in conjunction with the C-terminal NLS of nCLU) in transfected cells.

At the present time, little is known about the regulation of nCLU induction and translocation. Translocation of pnCLU from the cytoplasm to the nucleus was accompanied by an electrophoretic mobility shift of the nCLU protein (13). In its inactive form, pnCLU was an ~49-kDa protein present in the cytoplasm of control, non-irradiated MCF-7 cells; little, if any, protein was found in the nuclei of control MCF-7 cells (13). After IR exposure, ~55-kDa nCLU protein levels increased and translocated from the cytoplasm into the nuclei of damaged cells (13). The IR-induced, post-translational modification processes that activate nCLU are not known, but we hypothesize that these modifications are involved in exposing either of the functional NLS signals, allowing subsequent translocation of pnCLU to the nucleus, as the mature nCLU death protein (Fig. 9). It is also possible that other proteins may be involved as specific inhibitors of pnCLU maturation in much the same way as IκB blocks NF-κB activation (44). The nature of the apparent post-translational modification of pnCLU is not known, but mass spectrometry studies are ongoing to elucidate these modification processes.

Comparison of the subcellular distribution of GFP-nCLU and GFP-Center suggests that cytosolic pnCLU may be actively prevented from entering the nucleus or actively excluded. The non-coiled central region of the pnCLU protein (amino acids 98–317) appears to be responsible for the inhibition of nuclear import and the formation of the characteristic aggregates of nCLU in the cytoplasm; this region of the protein may bind to a certain cytosolic factor(s), may be required for oligomerization, or needed for folding of the pnCLU protein in the cytosol. The distinct nuclear localization of the End fragment of nCLU (aa 368–448) and significantly lower nuclear expression of the GFP-End NLS2mut (Fig. 7*G* and Fig. 8, *D* and *E*; Table II) indicate that the C-terminal NLS was the functional nuclear import sequence for nCLU. N-terminal NLS1 may contribute to the nuclear translocation of nCLU, but our data on Fig. 8, *B* and *C*, and Table II demonstrate that NLS1 function is not as prominent as that of NLS2.

Because the C-terminal coiled-coil domain of mouse nCLU (aa 318–367) did not have an apparent NLS, very little of the protein was detected in the nucleus of cells with apoptotic morphology. These data indicate that enough of this protein may have entered the nucleus due to forced, cytomegalovirus-directed overexpression to cause cell death. An alternative hypothesis is that the cell death function of nCLU may not require nuclear translocation. Our data suggest that dissocia-

tion of pnCLU coiled-coil domains may allow modification, translocation, and cell death responses. We are currently exploring the mechanism of nCLU transport into the nucleus, as well as the role of its nuclear internalization in nCLU-mediated cell death responses, including the apparent triggering of apoptotic responses.

Function of nCLU as a Death Gene—The precise intracellular functions of nCLU, as well as the significance of its binding to Ku70 protein, remain to be determined. As demonstrated in our previous (13) and current studies, overexpression of GFP-nCLU induces apoptosis in an apparent C-terminal coiled-coil- and NLS-dependent fashion. For example, overexpression of GFP-Ccoil, the Ku70-binding fragment of nCLU, resulted in short term apoptotic cytotoxicity (Fig. 7 and Table I), as well as long term clonogenic cytotoxicity (13). Although overall apoptosis measurements did not exceed 25–30% at any time, the clonogenic survival of the GFP-nCLU-positive MCF-7 cells was ~10-fold lower than GFP-alone transfected MCF-7 cells. Our data suggest, but do not prove, that interaction and interference with Ku70-dependent end joining, even in the absence of overt IR damage, can cause significant cell death. Superficially, this appears to mimic the enhanced apoptosis and lowered plating efficiency of $Ku70^{-/-}$ mouse embryonic fibroblasts (44). Elucidation of mechanisms by which *CLU* gene expression and nCLU production occur after DNA damage in tumor cells may augment various cancer therapies.

Acknowledgments—We thank Dr. John J. Pink for stimulating discussions and helpful suggestions, Dr. Martin Tenniswood for mouse CLU cDNA, Dr. M. Abe for mouse Ku70 cDNA, and Dr. Shinako Araki for help with confocal microscopy. We are also grateful to the Case Western Reserve University-University Hospital Comprehensive Cancer Center Radiation, Flow Cytometry, DNA Sequencing, and Confocal Core Facilities supported by NCI Grant P30 CA43703 from the National Institutes of Health.

REFERENCES

1. Danik, M., Chabot, J. G., Mercier, C., Benabid, A. L., Chauvin, C., Quirion, R., and Suh, M. (1991) *Proc. Natl. Acad. Sci. U. S. A.* **88,** 8577–8581
2. Bursch, W., Gleeson, T., Kleine, L., and Tenniswood, M. (1995) *Arch. Toxicol.* **69,** 253–258
3. Buttyan, R., Olsson, C. A., Pintar, J., Chang, C., Bandyk, M., Ng, P. Y., and Sawczuk, I. S. (1989) *Mol. Cell. Biol.* **9,** 3473–3481
4. Ahuja, H. S., Tenniswood, M., Lockshin, R., and Zakeri, Z. F. (1994) *Biochem. Cell Biol.* **72,** 523–530
5. Leger, J. G., Montpetit, M. L., and Tenniswood, M. P. (1987) *Biochem. Biophys. Res. Commun.* **147,** 196–203
6. Leger, J. G., Le Guellec, R., and Tenniswood, M. P. (1988) *Prostate* **13,** 131–142
7. May, P. C. (1993) *Ann. N. Y. Acad. Sci.* **679,** 235–244
8. Montpetit, M. L., Lawless, K. R., and Tenniswood, M. (1986) *Prostate* **8,** 25–36
9. Sensibar, J. A., Sutkowski, D. M., Raffo, A., Buttyan, R., Griswold, M. D., Sylvester, S. R., Kozlowski, J. M., and Lee, C. (1995) *Cancer Res.* **55,** 2431–2437
10. Tenniswood, M. P., Guenette, R. S., Lakins, J., Mooibroek, M., Wong, P., and Welsh, J. E. (1992) *Cancer Metastasis Rev.* **11,** 197–220
11. Wong, P. (1994) *Biochem. Cell Biol.* **72,** 489–498
12. Wong, P., Pineault, J., Lakins, J., Taillefer, D., Leger, J., Wang, C., and Tenniswood, M. (1993) *J. Biol. Chem.* **268,** 5021–5031
13. Yang, C. R., Leskov, K., Hosley-Eberlein, K., Criswell, T., Pink, J. J., Kinsella, T. J., and Boothman, D. A. (2000) *Proc. Natl. Acad. Sci. U. S. A.* **97,** 5907–5912
14. Yang, C. R., Yeh, S., Leskov, K., Odegaard, E., Hsu, H. L., Chang, C., Kinsella, T. J., Chen, D. J., and Boothman, D. A. (1999) *Nucleic Acids Res.* **27,** 2165–2174
15. Steinberg, J., Oyasu, R., Lang, S., Sintich, S., Rademaker, A., Lee, C., Kozlowski, J. M., and Sensibar, J. A. (1997) *Clin. Cancer Res.* **3,** 1707–1711
16. Miyake, H., Nelson, C., Rennie, P. S., and Gleave, M. E. (2000) *Cancer Res.* **60,** 2547–2554
17. Clark, A. M., and Griswold, M. D. (1997) *J. Androl.* **18,** 257–263
18. Kimura, K., Asami, K., and Yamamoto, M. (1997) *Cell Biochem. Funct.* **15,** 251–257
19. Michel, D., Chatelain, G., North, S., and Brun, G. (1997) *Biochem. J.* **328,** 45–50
20. Humphreys, D. T., Carver, J. A., Easterbrook-Smith, S. B., and Wilson, M. R. (1999) *J. Biol. Chem.* **274,** 6875–6881
21. Viard, I., Wehrli, P., Jornot, L., Bullani, R., Vechietti, J. L., Schifferli, J. A., Tschopp, J., and French, L. E. (1999) *J. Invest. Dermatol.* **112,** 290–296
22. Reddy, K. B., Jin, G., Karode, M. C., Harmony, J. A., and Howe, P. H. (1996) *Biochemistry* **35,** 6157–6163
23. Han, B. H., DeMattos, R. B., Dugan, L. L., Kim-Han, J. S., Brendza, R. P., Fryer, J. D., Kierson, M., Cirrito, J., Quick, K., Harmony, J. A., Aronow, B. J., and Holtzman, D. M. (2001) *Nat. Med.* **7,** 338–343
24. Tsuruta, J. K., Wong, K., Fritz, I. B., and Griswold, M. D. (1990) *Biochem. J.* **268,** 571–578
25. Alber, T. (1992) *Curr. Opin. Genet. & Dev.* **2,** 205–210
26. Hirai, S., and Yaniv, M. (1989) *New Biol.* **1,** 181–191
27. Kouzarides, T., Packham, G., Cook, A., and Farrell, P. J. (1991) *Oncogene* **6,** 195–204
28. Lupas, A., Van Dyke, M., and Stock, J. (1991) *Science* **252,** 1162–1164
29. Jordan-Starck, T. C., Lund, S. D., Witte, D. P., Aronow, B. J., Ley, C. A., Stuart, W. D., Swertfeger, D. K., Clayton, L. R., Sells, S. F., and Paigen, B., (1994) *J. Lipid Res.* **35,** 194–210
30. Flick, J. S., and Johnston, M. (1990) *Mol. Cell. Biol.* **10,** 4757–4769
31. Harper, J. W., Adami, G. R., Wei, N., Keyomarsi, K., and Elledge, S. J. (1993) *Cell* **75,** 805–816
32. Acharya, S., Wilson, T., Gradia, S., Kane, M. F., Guerrette, S., Marsischky, G. T., Kolodner, R., and Fishel, R. (1996) *Proc. Natl. Acad. Sci. U. S. A.* **93,** 13629–13634
33. Boothman, D. A., Bouvard, I., and Hughes, E. N. (1989) *Cancer Res.* **49,** 2871–2878
34. van Straaten, F., Muller, R., Curran, T., Van Beveren, C., and Verma, I. M. (1983) *Proc. Natl. Acad. Sci. U. S. A.* **80,** 3183–3187
35. Hope, I. A., and Struhl, K. (1985) *Cell* **43,** 177–188
36. Bohmann, D., Bos, T. J., Admon, A., Nishimura, T., Vogt, P. K., and Tjian, R. (1987) *Science* **238,** 1386–1392
37. Biggin, M., Bodescot, M., Perricaudet, M., and Farrell, P. (1987) *J. Virol.* **61,** 3120–3132
38. Flemington, E., and Speck, S. H. (1990) *Proc. Natl. Acad. Sci. U. S. A.* **87,** 9459–9463
39. Robbins, J., Dilworth, S. M., Laskey, R. A., and Dingwall, C. (1991) *Cell* **64,** 615–623
40. Harmony, J. A. K. (ed) (1995) *Clusterin: Role in Vertebrate Development, Function, and Adaptation,* pp. 75–100, R. G. Landes Co., Springer-Verlag, Heidelberg, Germany
41. Simboli-Campbell, M., Narvaez, C. J., Tenniswood, M., and Welsh, J. (1996) *J. Steroid Biochem. Mol. Biol.* **58,** 367–376
42. Leskov, K. S., Criswell, T., Antonio, S., Li, J., Yang, C. R., Kinsella, T. J., and Boothman, D. A. (2001) *Semin. Radiat. Oncol.* **11,** 352–372
43. Koch-Brandt, C., and Morgans, C. (1996) *Prog. Mol. Subcell. Biol.* **16,** 130–149
44. Kim, S. H., Kim, D., Han, J. S., Jeong, C. S., Chung, B. S., Kang, C. D., and Li, G. C. (1999) *Cancer Res.* **59,** 4012–4017
45. Walker, J. R., Corpina, R. A., and Goldberg, J. (2001) *Nature* **412,** 607–614